New Design Techniques for Efficient Arithmetization-Oriented Hash Functions: `Anemoi` Permutations and `Jive` Compression Mode

Clémence Bouvier[1,2], Pierre Briaud[1,2], Pyrros Chaidos[3], Léo Perrin[2], Robin Salen[4], Vesselin Velichkov[5,6], Danny Willems[7,8]

[1] Sorbonne University, France,
[2] Inria, France
[3] National & Kapodistrian University of Athens, Greece,
[4] Toposware, Inc., USA
[5] University of Edinburgh, Scotland
[6] Clearmatics, England
[7] Nomadic Labs, France
[8] LIX, France
anemoi@inria.fr

Abstract. Advanced cryptographic protocols such as Zero-knowledge (ZK) proofs of knowledge, widely used in cryptocurrency applications such as Zcash, Monero, Filecoin, demand new cryptographic hash functions that are efficient not only over the binary field $\mathbb{F}_2$, but also over large fields of prime characteristic $\mathbb{F}_p$. This need has been acknowledged by the wider community and new so-called *Arithmetization-Oriented* (AO) hash functions have been proposed, e.g. MiMC-Hash, Rescue–Prime, Poseidon, `Reinforced Concrete` and Griffin to name a few.

In this paper we propose `Anemoi`: a new family of ZK-friendly permutations, than can be used to construct efficient hash functions and compression functions. The main features of these algorithms are that 1) they are designed to be efficient within multiple proof systems (e.g. Groth16, Plonk, etc.), 2) they contain dedicated functions optimised for specific applications (namely Merkle tree hashing and general purpose hashing), 3) they have highly competitive performance e.g. about a factor of 2 improvement over Poseidon and Rescue–Prime in terms of R1CS constraints, a 28%-48% Plonk constraint reduction over a highly optimized Poseidon implementation, as well as competitive native performance, running between two and three times faster than Rescue–Prime, depending on the field size.

On the theoretical side, `Anemoi` pushes further the frontier in understanding the design principles that are truly entailed by arithmetization-orientation. In particular, we identify and exploit a previously unknown relationship between CCZ-equivalence and arithmetization-orientation. In addition, we propose two new standalone components that can be easily reused in new designs. One is a new S-box called `Flystel`, based on the well-studied butterfly structure, and the second is Jive – a new mode of operation, inspired by the "Latin dance" symmetric algorithms (Salsa, ChaCha and derivatives).

Keywords: Anemoi · Flystel · Jive · Arithmetization-oriented · Hash functions · CCZ-equivalence · Plonk · R1CS · AIR · Merkle tree · Zero-knowledge · Arithmetic circuits

1 Introduction

In recent years we have seen a rapid surge of interest in the practical application of an old cryptographic construction known as zero-knowledge (ZK) proofs of knowledge. Such protocols allow a prover P to convince a verifier V that a certain statement x is true without revealing any additional information beyond the fact that it is verifiably correct. Such a piece of information may, for example, be that the result of a specified complex computation is 1. With a ZK protocol, V can verify that the result of this computation is correct without having to perform the computation herself. In fact, to verify correctness V does not even need to know some of the details of the computation e.g. its intermediate values or any potentially secret inputs.

ZK proof systems have been introduced with the seminal work of Micali, Goldwasser and Rackoff back in 1989 [GMR89]. Traditionally, ZK protocols were deployed to allow a prover to keep some elements of a computation secret (e.g. a private key). More recently, the blockchain ecosystem has witnessed a rise of a category of ZK protocols, namely Succinct Non-Interactive Arguments of Knowledge (ZK-SNARKs), that leverages their succinctness property to relieve the verifier from the necessity to perform an expensive computation for which it may not have sufficient resources (in terms of space as well as computational power). The increased interest in such protocols today is largely driven by the latest advancements in digital currencies such as Bitcoin, Ethereum, etc. In particular, ZK proofs make it possible to add privacy on a public blockchain (e.g. Zcash [BSCG+14]) and to perform off-chain computation verifiable by network nodes with significantly limited resources, improving scalability.

The computation performed by P and verified by V in a ZK proof is often expressed as an arithmetic circuit composed of *gates* (algebraic operations e.g. multiplication or addition) connected by *wires*. The quantities that pass over the wires and are operated on by the gates are elements of a field $\mathbb{F}_q$, where $q \geq 2$.

Cryptographic hash functions are fundamental to practical ZK applications. They are often used for testing membership of some element(s) by means of Merkle trees. They can also be used as part of the ZK protocol itself e.g. by compressing multiple public inputs to a single hash. The modified protocol has a reduced input footprint, and the collision resistance of the hash function implies that security is not impacted. This is relevant in proof systems where the verifier's costs are proportional to the number of public inputs such as Groth16 [Gro16].

Modern cryptographic hash functions such as SHA2, SHA3 and BLAKE are designed over vector spaces of the binary field $\mathbb{F}_2$ (i.e. they work over bits), while ZK protocols often operate over $\mathbb{F}_q$ for a large q – usually a prime number. Therefore the efficient execution of ZK protocols in applications such as Zcash or Filecoin, that aim to process millions of transactions per day, imposes the need for new hash functions designed to be natively efficient in $\mathbb{F}_q$ – the so-called *Arithmetization-Oriented* (AO) designs. The need for new arithmetization-oriented hash functions has been acknowledged by both researchers and engineers. As a result, the past couple of years have seen a surge of new proposals of hash functions that operate natively in $\mathbb{F}_q$ for q prime, enabling efficient verification: MiMC-Hash [AGR+16], Poseidon [GKR+21], Rescue–Prime [AAB+20, SAD20], Reinforced Concrete [BGK+21] and Griffin [GHR+22] to name a few.

The Design Requirements of Arithmetization-Orientation. Building upon the works mentioned above as well as on the study of practical use cases, we have identified several properties and design requirements that are expected from arithmetization-oriented hash function.

Evaluation vs. Verification. The operation for which the efficiency of an AO primitive is the most crucial is not its *evaluation*, but rather its *verification*. Concretely, while the cost of evaluating $y = F(x)$ given x remains important, the step with the harshest constraints is a verification: given both x and y, checking if y is indeed equal to $F(x)$ should be "efficient", where the exact meaning of "efficient" depends on the proof system considered.

b-to-1 compression. One of the main use cases for AO hash functions is in Merkle trees. In this context, rather than a hash function taking arbitrarily long inputs, protocol designers need a compression function mapping bm to m finite field elements, meaning a compression factor of b (often, $b = 2$).

Primitive Factories. Rather than a single primitive or a small family of primitives (such as for instance AES-128/192/256), AO hash functions are defined for a vast number of field sizes and security levels. In fact, we would argue that algorithms like POSEIDON are *primitive factories*[1], and that the task of the cryptanalysts is not only to assess whether specific instances are secure. Rather, it is to verify if such factories can return weak algorithms. Furthermore, since the protocols and arihmetization techniques vary, a factory should be able to output primitives optimized for each use case.

Performance constraints. The space and time complexities of the proving systems depend on the arithmetized program size (i.e. the number of gates) to be verified, meaning that it is crucial for practical applications to minimize the number of gates, as the cost of a proof may otherwise be so high as to make it unusable, as the computational cost of the prover becomes the bottleneck of an entire system. AIR-based systems additionally require keeping constraint degrees low for practical applications. Furthermore, good conventional CPU architecture performance is still required as real world applications tend to use the primitives both outside and inside the circuit.

Outine of our Contributions. In this paper, we study each of the specific design requirements of AO, and provide new tools to satisfy them. First, we present the necessary theoretical background in Section 2.

We then present two building blocks. First, in Section 3 we introduce a new mode of operation, Jive, which turns a public permutation into a t-to-1 compression function. Its main advantage is that it compresses an input consisting of tu words using a permutation operating on a state consisting of tu words, unlike the sponge structure which needs a bigger state in order to accomodate a capacity. Then, in Section 4, we argue that the asymmetry between the evaluation and the verification of a function is best framed in terms of *CCZ-equivalence*. Using this insight, we propose a new family of non-linear components (S-boxes) operating on $\mathbb{F}_q^2$ which we called `Flystel`: they allow both a high degree evaluation, and a low degree verification.

In a natural progression, we use the `Flystel` structure to construct a new permutation factory: `Anemoi`. It uses the familiar Substitution-Permutation Network (SPN) structure, which simplifies our security analysis. Its specification is given in Section 5, and our initial cryptanalysis is presented in Section 6. We combine all these results together in Section 7, where we show via detailed benchmarks that combining the `Anemoi` permutations with the Jive mode of operation allows us to compete with the best AO hash functions in the literature in terms of performance, and to substantially outclass them in some contexts. In particular, in the case of Plonk, we can compute more than twice as many hashes for a fixed number of constraints as is possible with POSEIDON, which to the best of our knowledge was the best until now. We conclude the paper in Section 8.

[1]"Factory" is here used in the sense of the programming design pattern, i.e. it is an object returning functions.

2 Theoretical Background

In what follows, q is an integer corresponding to the size of the field $\mathbb{F}_q$, so that $q = p$ for some prime number p or $q = 2^n$. As usual, the symbols "+" and "×" denote respectively the addition and the multiplication over $\mathbb{F}_q$. We also let $m \geq 1$ be an integer corresponding to the number of field elements we are operating on. We denote $\langle a, b\rangle$ the usual scalar product of $a \in \mathbb{F}_q^m$ and $b \in \mathbb{F}_q^m$ which is such that $\langle a, b\rangle = \sum_{i=0}^{m-1} a_i b_i$.

Below, we consider a function $F : \mathbb{F}_q^m \to \mathbb{F}_q^m$, and recall some of the concepts behind the use and analysis of functions to design symmetric cryptographic primitives. We first recall the definition of their differential and linear properties, and then that of *CCZ-equivalence*. While the latter was seldom used in practice so far, it plays a crucial role in our work.

Differential Properties. The *Difference Distribution Table (DDT)* of function F is the two dimensional array δ_F, where $\delta_F[a, b] = \#\{x \in \mathbb{F}_q^m | F(x+a)-F(x) = b\}$. The maximum value of $\delta_F[a, b]$ for $a \neq 0$ is the *differential uniformity* [Nyb94] of F.

Linear Properties. While a general formula that works both when q is a power of two and a prime can be given, it is simpler to treat the two cases separately, especially given that the reader is probably familiar with the case of characteristic 2. If $q = 2^n$, then the Walsh transform of the component $\langle b, F\rangle : \mathbb{F}_q \to \mathbb{F}_2$ for any $b \in \mathbb{F}_q \backslash \{0\}$ is $\mathcal{W}_{\langle b,F\rangle}(a) = \sum_{x\in\mathbb{F}_2^m} (-1)^{\langle a,x\rangle+\langle b,F(x)\rangle}$.

Otherwise, when $q = p$ the Fourier transform of a function $f : \mathbb{F}_p^m \to \mathbb{F}_p$ is the function $\mathcal{W}_f : \mathbb{F}_p^m \to \mathbb{C}$ such that

$$\mathcal{W}_f(a) = \sum_{x\in\mathbb{F}_p^m} \exp\left(\frac{2\pi i\left(\langle a, x\rangle - f(x)\right)}{p}\right) .$$

For a vectorial function $F : \mathbb{F}_q^m \to \mathbb{F}_q^m$, we consider the Fourier transform of each of its components, i.e. of all the linear combinations $\langle b, F\rangle$.

CCZ-Equivalence [CCZ98]. Let $F : \mathbb{F}_q^m \to \mathbb{F}_q^m$ and $G : \mathbb{F}_q^m \to \mathbb{F}_q^m$ be two functions. They are *affine-equivalent* if there exists two affine permutation $\mu : \mathbb{F}_q^m \to \mathbb{F}_q^m$ and $\eta : \mathbb{F}_q^m \to \mathbb{F}_q^m$ such that $F = \eta \circ G \circ \mu$. This can alternatively be written using the *graphs* of these functions:

$$\Gamma_F = \underbrace{\left\{ (x, F(x)) \mid x \in \mathbb{F}_q^m \right\}}_{\text{graph of } F} = \mathcal{L}(\Gamma_G) = \left\{\mathcal{L}\left(x, F(x)\right) \mid x \in \mathbb{F}_q^m\right\} ,$$

where $\mathcal{L}$ is the affine permutation defined by $\mathcal{L}(x, y) = \big(\eta(x), \mu^{-1}(y)\big)$. If we allow $\mathcal{L}$ to be any affine permutation,[2] we obtain *CCZ-equivalence*.

Definition 1 (CCZ-Equivalence)**.** Let F and G be functions of $\mathbb{F}_q^m$. We say that they are *CCZ-equivalent* if there exists an affine permutation $\mathcal{L} : (\mathbb{F}_q^m)^2 \to (\mathbb{F}_q^m)^2$ such that $\Gamma_F = \mathcal{L}(\Gamma_G)$.

An important property of CCZ-equivalence that is instrumental in our work is that it preserves the differential spectrum and the squared Walsh coefficients. In other words, all functions within the same CCZ-equivalence class share the same differential and linear properties and hence offer the same resilience against differential and linear attacks. It

[2] Starting from a given function F, applying any affine permutation of $\mathbb{F}_q^2$ to its graph is unlikely to yield the graph of another function G. Indeed, this would require that the left hand side of $\mathcal{L}(x, F(x))$ takes all the values in $\mathbb{F}_q$ as x goes through $\mathbb{F}_q$, which is a priori not the case. A mapping $\mathcal{L}$ that does yield the graph of another function is called "admissible", a concept that was extensively studied in [CP19].

also means that it is sufficient to investigate these properties for a single member of a CCZ-equivalence class.

Another relevant property of CCZ-equivalence is that it does *not* preserve the degree of the function. In fact, there are known cases where a low-degree function is CCZ-equivalent to a higher-degree one. It is most notably the case of the so-called *butterfly structure*, originally introduced in [PUB16], and then further generalized in two different ways in [CDP17] and [LTYW18].

3 Modes of Operation

In advanced protocols, hash functions are used for two purposes. The first is to emulate a random oracle, in particular to return the "fingerprint" or digest of a message of arbitrary length. The idea is that this fixed length digest is simpler to sign than the full message. The second use is as a compression function within a Merkle-tree: in this case, the hash function H is used to map two inputs of size n to an output of size n, and the security of the higher level scheme relies on its collision resistance. While a general purpose hash function like `SHA-3` [BDPA13, Dwo15] or an arithmetization-friendly one can safely be used for both uses, for improved efficiency we chose to use a full hash function only for the random oracle case (Section 3.1). Indeed, the specific constraints of the Merkle-tree case can be satisfied more efficiently using a dedicated structure that remains permutation-based, and which we introduce in Section 3.2. SAGE implementations of both modes are provided in Appendix C.

3.1 Random Oracle: the Sponge Structure

A random oracle is essentially a theoretical function that picks each output uniformly at random while keeping track of its previous outputs in order to remain a deterministic function. The sponge construction is a convenient approach to try to emulate this behaviour. First introduced by Bertoni et al. in [BDPVA07], this method was most notably used to design SHA-3. It is also how most arithmetization-oriented hash functions have been designed, e.g. Rescue–Prime, gMiMC-Hash, Poseidon [GKR+21], and `Reinforced Concrete`. Such hash functions can easily be tweaked into eXtendable Output Functions (XOF) [Dwo15] should the need arise.

The overall principle of the sponge construction is best explained by the diagram in Figure 1. In this paper, we slightly modify the original approach to operate on elements of $\mathbb{F}_q$ instead of $\mathbb{F}_2$. The main component of the structure is a permutation P operating on $\mathbb{F}_q^{r+c}$, where both r and c are non-zero integers. The *rate* r is the size of the *outer part* of the state, while c is the *capacity* and corresponds to the size of the *inner part* of the state. The digest consists of h elements of $\mathbb{F}_q$. Then, to process a message m consisting of elements of $\mathbb{F}_q$, we apply the following operations.

Padding. A basic padding works as follows: append $1 \in \mathbb{F}_q$ to the message followed by enough zeroes so that the total length is a multiple of r, and then divide the result into blocks $m_0,...,m_{\ell-1}$ of r elements.

However, with this approach, we may end up using one more call to P in the case where the length of the message was already a multiple of r. A more efficient approach is presented in [Hir16]: if the length of the message is already a multiple of r, then we do not append further blocks to it. Instead, we add a constant to the capacity before squeezing. This is summarized as the addition of σ which is equal to 0 if the message length is not a multiple of r, and to 1 otherwise (see Figure 1). This variant also has the advantage of gracefully handling the case where $r = 1$.

Absorption. For each message block m_i, we add it into the outer part of the state, and then apply P on the full state.

Squeezing. We extract $\min(h, r)$ elements from the outer part of the state to generate the first elements of the digest. If $h > r$, we apply P and then extract additional elements again from the rate registers, repeating this process until the desired digest length is reached.

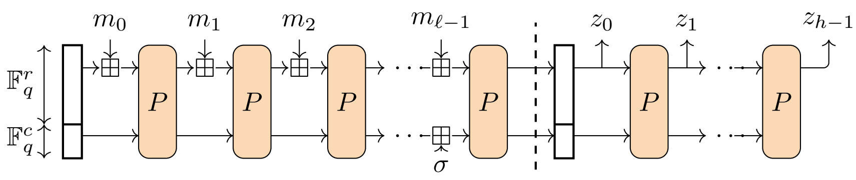

Figure 1: *Sponge construction with the modification of [Hir16].*

The security of a sponge rests on the properties of its permutation. Informally, the only special property of the permutation should be the existence of an efficient implementation. Its differential, linear, algebraic, etc. properties should be similar to those expected from a permutation picked uniformly at random from the set of all permutations.

Following a *flat sponge claim* [BDPVA07], the designers of such an algorithm can essentially claim that any attack against it will have a complexity equivalent to at least $q^{c/2}$ calls to the permutation (provided that $h \geq c$). Thus, a flat sponge claim states that a sponge-based hash function provides $nc/2$ bits of security.

3.2 Merkle Compression Function: the Jive Mode

One of the main use cases for an arithmetization-oriented hash function is as a compression function in a Merkle tree. This case could be easily handled using a regular hashing mode, such as the sponge structure discussed above. However, due to the specifics of this use case, it is possible to use a more efficient mode.

In a Merkle tree, the elements considered are in $\mathbb{F}_q^m$, where m is chosen so that $m\lfloor\log_2 q\rfloor \geq n$, where n is the intended security level. We then need to hash two such elements to obtain a new one. As a consequence, unlike in the usual case, the input size is fixed, and is equal to exactly twice the digest size. Given a permutation of $(\mathbb{F}_q^m)^2$, we can thus construct a suitable hash function by plugging it into the following mode.

Definition 2 (Jive)**.** Consider a permutation P defined as follows:

$$P : \begin{cases} (\mathbb{F}_q^m)^b & \to (\mathbb{F}_q^m)^b \\ (x_0, ..., x_{b-1}) & \mapsto (P_0(x_0, ..., x_{b-1}), ..., P_{b-1}(x_0, ..., x_{b-1})) \end{cases} ,$$

so that it operates on bm of elements of $\mathbb{F}_q$, where $P_i(x_0, \ldots, x_{b-1}) : 0 \leq i < b$ refers to the i-th element in $\mathbb{F}_q^m$ of the output $P(x_0, \ldots, x_{b-1})$ from P. The mode Jive is built from P by defining the following one way function $\mathsf{Jive}_b(P)$:

$$\mathsf{Jive}_b(P) : \begin{cases} (\mathbb{F}_q^m)^b & \to \mathbb{F}_q^m \\ (x_0, ..., x_{b-1}) & \mapsto \sum_{i=0}^{b-1} (x_i + P_i(x_0, ..., x_{b-1})) \end{cases} .$$

This approach can be seen as a permutation-based variant of the Davies-Meyer mode which, like the latter, crucially relies on a feed-forward to ensure one-wayness. Alternatively, it can be interpreted as a truncated instance of the mode used in the “Latin dance” ciphers

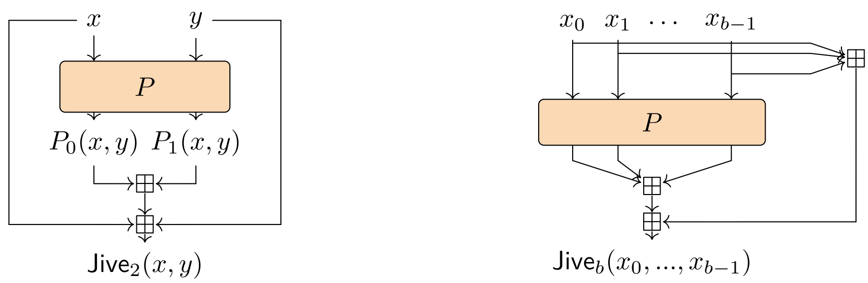

(a) Jive_2*, which maps* $(\mathbb{F}_q^m)^2$ *to* $\mathbb{F}_q^m$*.* **(b)** Jive_b*, which maps* $(\mathbb{F}_q^m)^b$ *to* $\mathbb{F}_q^m$*.*

Figure 2: *The* Jive *mode turning a permutation into a compression function.*

ChaCha and Salsa [Ber08], which is also based on a public permutation combined with a feedforward. Incidentally, we called it Jive after another Latin dance.

If used inside a Merkle tree, this mode can save some computations. For example, in the case where the fan-in b is equal to 2, a sponge would use a permutation operating on $(\mathbb{F}_q^m)^3$ in order to leave one vector of $\mathbb{F}_q^m$ free for the capacity. Using Jive_2 instead, we only need a permutation of $(\mathbb{F}_q^m)^2$. The trade-off of course is that, unlike a sponge-based approach, the relevance of Jive is restricted to some specific cases.

4 The `Flystel` Structure

The performance metrics for AO algorithms differ substantially from the usual ones in symmetric cryptography. Neither the number of CPU cycles, nor the RAM consumption or the code size are the dominant factors. At the same time, pin-pointing exactly what is needed for the various protocols relying on arithmetization is a difficult task as each protocol has its own subtleties. For example, Plonk offers custom gates, which are difficult to develop but can decrease the overall cost of an operation, while other proof systems might not. On the other hand, additions are essentially free for R1CS or AIR, but not for Plonk. In addition, permutations of a sequence of field elements are likely to incur cost in Plonk or AIR (in the form of copy-constraints), but are free in R1CS.

In this section, we present a family of non-linear components that provide both the cryptographic properties that we need to ensure the security of our primitives, and efficient implementations across proof systems, which we call *open* ***`Flystel`***. It uses—and highlights—the connection between arithmetization-orientation and CCZ-equivalence.

4.1 On CCZ-Equivalence and Arithmetization-Orientation

In order for a function F to be arithmetization-oriented, it is necessary that verifying whether $y = F(x)$ can be done using few multiplications in a specific field (whose size is dictated by other parts of the protocol). A very straight-forward initial approach is to use a function F which, itself, can be evaluated using a small number of multiplications: both MiMC-Hash [AGR+16] and Poseidon [GKR+21] work in this way. The downside is that using a low degree round function may imply vulnerability to attacks based on polynomial solving, known as *algebraic attacks*. As a consequence, these algorithms have to use a high number of rounds.

A first breakthrough on this topic was made by the designers of Rescue–Prime [AAB+20]. They noticed that for a permutation F, checking if $y = F(x)$ is equivalent to checking if $x = F^{-1}(y)$. It allows them to use both x^α and $x^{1/\alpha}$ (where $x \mapsto x^\alpha$ is a permutation of the field used) in their round function, with α chosen so as to minimize the number of

(a) *Open* `Flystel`*,* $\mathcal{H}$*.* **(b)** *Closed* `Flystel`*,* $\mathcal{V}$*.*

Figure 3: *The* `Flystel` *structure (both variants are CCZ-equivalent).*

multiplications. It means that both can be verified using a (cheap) evaluation of x^α, and at the same time that the degree of the round function is very high as $1/\alpha$ is a dense integer of $\mathbb{Z}/(q-1)\mathbb{Z}$. As a consequence, much fewer rounds are needed to prevent algebraic attacks.

We go further and propose a generalization of this insight. So far, we have seen that AO implies that a function or its inverse must have a particular implementation property (low number of multiplications). In fact, we claim the following:

> A subfunction is arithmetization-oriented if it is **CCZ-equivalent** to a function that can be verified efficiently.

The above should come as no surprise since a permutation and its inverse are known to be CCZ-equivalent [BCP06]. In that sense, this insight is a natural generalization of the one of the Rescue–Prime designers.

Exploiting this idea is simple: suppose that F and G are such that $\Gamma_F = \mathcal{L}(\Gamma_G)$, where $\mathcal{L} : (x, y) \mapsto (\mathcal{L}_L(x, y), \mathcal{L}_R(x, y))$ is an affine permutation, and where G can be efficiently verified. Then we can use F to construct an AO algorithm: checking if $y = F(x)$ is equivalent to checking if $\mathcal{L}_L(x, y) = G(\mathcal{L}_R(x, y))$, which only involves G and linear functions: it is efficient.

Below, we present a first component based on this idea: the `Flystel`. Nevertheless, we hope that further research in discrete mathematics will lead to new non-linear components that are even better suited to this use case: we need more permutations with good cryptographic properties (including a high degree) that are CCZ-equivalent to functions with a low number of multiplications.

4.2 High Level View of the `Flystel` Structure

Let $Q_\gamma : \mathbb{F}_q \to \mathbb{F}_q$ and $Q_\delta : \mathbb{F}_q \to \mathbb{F}_q$ be two quadratic functions, and let $E : \mathbb{F}_q \to \mathbb{F}_q$ be a permutation. Then, the ***`Flystel`*** is a pair of functions relying on Q_γ, Q_δ and E. The *open* ***`Flystel`*** is the permutation of $(\mathbb{F}_q)^2$ obtained using a 3-round Feistel network with Q_γ, E^{-1}, and Q_δ as round functions, as depicted in Figure 3a. It is denoted $\mathcal{H}$, so that $\mathcal{H}(x, y) = (u, v)$ is evaluated as follows:

1. $x \leftarrow x - Q_\gamma(y)$,
2. $y \leftarrow y - E^{-1}(x)$,
3. $x \leftarrow x + Q_\delta(y)$,
4. $u \leftarrow x,\ v \leftarrow y$.

The *closed* ***`Flystel`*** is a function of $\mathbb{F}_q^2$ defined by $\mathcal{V} : (y, v) \mapsto (R_i(y, v), R_f(v, y))$, where $R_j : (y, v) \mapsto E(y - v) + Q_j(y)$ for $j \in \{i, f\}$.

Our terminology of "open" for the permutation and "closed" for the function is based on the relation between the `Flystel` and the butterfly structure, as detailed later. In particular, the two `Flystel`s are linked in the following way.

Proposition 1. *For a given tuple (Q_γ, E, Q_δ), the corresponding closed and open `Flystel` are CCZ-equivalent.*

Proof. Let $(u, v) = \mathcal{H}(x, y)$. Then it holds that $v = y - E^{-1}(x - Q_\gamma(y))$, so that we can write $x = E(y - v) + Q_\gamma(y)$. Similarly, we have that $u = Q_\delta(v) + E(y - v)$. Consider now the set $\Gamma_\mathcal{H} = \{((x, y), \mathcal{H}(x, y)), (x, y) \in \mathbb{F}_q^2\}$. By definition, we have

$$\Gamma_\mathcal{H} = \{((x, y), (u, v)), (x, y) \in \mathbb{F}_q^2\} = \mathcal{L}\big(\{((y, v), (x, u)), (x, y) \in \mathbb{F}_q^2\}\big)$$

where $\mathcal{L}$ is the permutation of $(\mathbb{F}_q^2)^2$ such that $\mathcal{L}((x, y), (u, v)) = ((y, v), (x, u))$, which is linear. Using the equalities we established at the beginning of this proof, we can write:

$$\begin{aligned}\mathcal{L}^{-1}(\Gamma_\mathcal{H}) &= \{((y, v), (x, u)), (x, y) \in \mathbb{F}_q^2\} \\ &= \{\big((y, v), (Q_\gamma(y) + E(y - v), Q_\delta(v) + E(y - v))\big), (y, v) \in \mathbb{F}_q^2\} = \Gamma_\mathcal{V} .\end{aligned}$$

We deduce that $\Gamma_\mathcal{H} = \mathcal{L}(\Gamma_\mathcal{V})$, so the two functions are CCZ-equivalent. □

This simple proposition has two crucial corollaries on which we will rely in the remainder of the paper. The first is that it suffices to investigate the differential and linear properties of the closed butterfly to obtain results on the open one.

Corollary 1. *The open and closed `Flystel` structures have identical differential and linear properties. More precisely, the set of the values in the DDT of both functions is the same, and the set of the square of the Fourier coefficients of the components is also the same.*

The second corollary is the key reason behind the relevance of the `Flystel` structure in the airthmetization-oriented setting and is stated below.

Corollary 2. *Verifying that $(u, v) = \mathcal{H}(x, y)$ is equivalent to verifying that $(x, u) = \mathcal{V}(y, v)$.*

Indeed, Corollary 2 means that it is possible to encode the verification of the evaluation of the high degree open `Flystel` using the polynomial representation of the low degree closed `Flystel`.

In characteristic 2, quadratic mappings correspond to different exponents than in the general case. As a consequence, when giving concrete instanciations of the `Flystel` structure, we need to treat this case separately. To highlight the difference, we call $\texttt{Flystel}_2$ the instances used in characteristic 2, and $\texttt{Flystel}_\texttt{p}$ the instances used in odd prime characteristic.

4.3 Characteristic 2

Let $q = 2^n$, with n odd. Furthermore, let $\alpha = 2^i + 1$ be such that $\gcd(i, n) = 1$, so that $x \mapsto x^\alpha$ is a permutation of $\mathbb{F}_q$. In this case, the $\texttt{Flystel}_2$ structure with $Q_\gamma(x) = Q_\delta(x) = \beta x^\alpha$, with $\beta \neq 0$, and with $E(x) = x^\alpha$ is a degenerate generalized butterfly structure. It was studied in [LTYW18] as a generalization of the structure introduced in [PUB16], which was also refined in [CDP17]. We recall the following particular case[3] in Theorems 3, 4 and 5 of [LTYW18].

Proposition 2 ([LTYW18])**.** *Let $q = 2^n$ with n odd, $E = x \mapsto x^\alpha$, where $\alpha = 2^i + 1$ is such that $\gcd(i, n) = 1$, and $Q_\gamma = Q_\delta = x \mapsto \beta x^\alpha$, where $\beta \neq 0$. Then the $\texttt{Flystel}_2$ structures defined by the functions Q_γ, E, and Q_δ have differential uniformity equal to 4, linearity equal to $2^{2n-1} - 2^n$, and algebraic degree of n.*

[3]The result of Li et al. covers all generalized butterflies, not just those corresponding to `Flystel` structures. In a `Flystel`, the first parameter (which we will denote a) is set to 1. Their results for the differential uniformity and the linearity holds only when $\beta \neq (1 + a)^\alpha$, meaning that we simply need to make sure that $\beta \neq 0$. For the algebraic degree, the condition they give in their Theorem 5 to have a degree equal to $n + 1$ degenerates into $\beta^{2^{i+1}} = \beta^{2^i+1}$, which is never the case as $i > 0$.

In practice, to prevent some attacks (see Section A.3), we instead use $Q_\gamma(x) = \beta x^3 + \gamma$ and $Q_\delta(x) = \beta x^3 + \delta$, where γ and δ are constants of $\mathbb{F}_q$ such that $\gamma \neq \delta$. The resulting construction is depicted in Figure 4a.

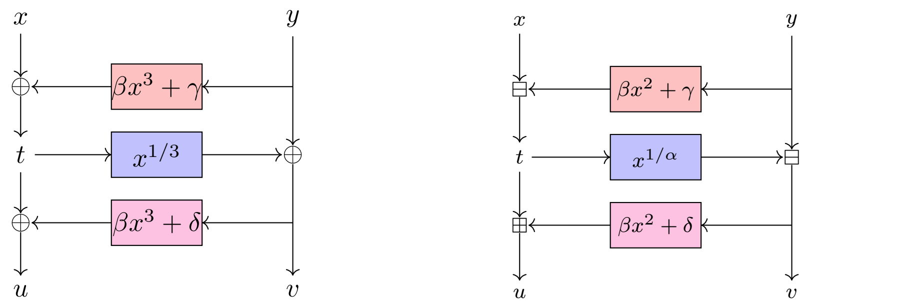

(a) *$\mathtt{Flystel}_2$ in characteristic 2.* **(b)** *$\mathtt{Flystel}_p$ in odd prime characteristic.*

Figure 4: *The two variants of the open* **Flystel**, *mapping (x, y) to (u, v).*

4.4 Odd Characteristic

When $q = p$, the $\mathtt{Flystel}_\mathtt{p}$ structure uses three rounds functions: $Q_\gamma : x \mapsto \beta x^2 + \gamma$, $E : x \mapsto x^{1/\alpha}$, and $Q_\delta : x \mapsto \beta x^2 + \delta$, where $\alpha, \beta, \gamma \in \mathbb{F}_q$ and $\beta \neq 0$.

Differential Properties. Such structures have a low differential uniformity.

Proposition 3. *Let $q = p$ be a prime number, $E = x \mapsto x^\alpha$, where α is such that* $\gcd(\alpha, p - 1) = 1$*, and $Q_\gamma = x \mapsto \gamma + \beta x^2$, $Q_\delta = x \mapsto \delta + \beta x^2$ where $\beta \neq 0$. Then the $\mathtt{Flystel}_p$ structures defined by the functions Q_γ, E, and Q_δ has a differential uniformity equal to $\alpha - 1$.*

Proof. Let a, b, c, d be elements of $\mathbb{F}_p$ such that $(a, b) \neq (0, 0)$. To investigate the differential uniformity of $\mathcal{V} : (y, v) \mapsto (R_i(y, v), R_f(v, y))$, we look at the number of solutions (y, v) of (1).

$$\begin{cases} R_i(y + a, v + b) - R_i(y, v) = c \\ R_f(v + b, y + a) - R_f(v, y) = d \ . \end{cases} \tag{1}$$

We have:

$$\begin{cases} R_i(y + a, v + b) - R_i(y, v) = (y + a - (v + b))^\alpha + \gamma + \beta(v + b)^2 - (y - v)^\alpha - \gamma - \beta v^2 \\ R_f(v + b, y + a) - R_f(v, y) = (v + b - (y + a))^\alpha + \delta + \beta(y + a)^2 - (v - y)^\alpha - \delta - \beta y^2 \ . \end{cases}$$

As α is odd, we deduce:

$$\begin{cases} R_i(y + a, v + b) - R_i(y, v) = (y + a - (v + b))^\alpha + \beta(v + b)^2 - (y - v)^\alpha - \beta v^2 \\ R_f(v + b, y + a) - R_f(v, y) = -(y + a - (v + b))^\alpha + \beta(y + a)^2 + (y - v)^\alpha - \beta y^2 \ . \end{cases}$$

Noting respectively ℓ_1 and ℓ_2 the rows of the system, we get:

$$\ell_1 + \ell_2 = \beta(v + b)^2 - \beta v^2 + \beta(y + a)^2 - \beta y^2 = c + d \ ,$$

which is equivalent to:

$$v = (2b)^{-1} \left(\beta^{-1}(c + d) - (2ay + a^2 + b^2)\right) \ .$$

As a consequence, we know that v can be expressed as an affine polynomial in y. So, we have

$$\ell_2 = -(y + a - (v + b))^\alpha + \beta(y + a)^2 + (y - v)^\alpha - \beta y^2$$

Recalling that v is of degree 1 in y, we have that ℓ_2 is an equation in y of degree $\alpha - 1$ (since the terms y^α cancel out), and thus at most $\alpha - 1$ solutions for y. In the end, we have at most $\alpha - 1$ solutions (y, v) for the system (since for each value of y, there is one v). □

Linear Properties. We do not have a theoretical bound on the correlation for the $\texttt{Flystel}_\texttt{p}$ structure, but we provide informal arguments supporting its security against linear cryptanalysis attacks. Notice first that $\texttt{Flystel}_\texttt{p}$ is defined by the functions Q_γ, E^{-1} and Q_δ, where Q_γ and Q_δ are quadratic. Given that the function x^2 is bent (i.e. its correlations are the lowest possible), we argue that a linear trail which would activate just one of these functions should be expected to have a very low correlation. In Appendix A, we give a conjecture supported by experimental results, stating that the linearity of $\texttt{Flystel}_\texttt{p}$ is lower than $p \log p$.

Invariant Subset. Regardless of the characteristic, it holds that $\mathcal{H}\left(Q_\gamma(x), x\right) = (Q_\delta(x), x)$. Thus, setting $Q_\gamma = Q_\delta$ would mean that `Flystel` is the identity over a subset of size q, which is why we use constant additions to ensure $Q_\gamma \neq Q_\delta$. Nevertheless, this only ensures that the open `Flystel` is a translation over the set $\{(Q_\gamma(x), x), x \in \mathbb{F}_q\}$, which remains cryptographically weak. While a priori undesirable, the impact of this property can be mitigated. First, the subset over which it has a simple expression is not an affine space. Second, as we show in Appendix A.3, the propagation of such patterns can be broken via the linear layer.

Degree. Given the structure of the open $\texttt{Flystel}_\texttt{p}$, its degree is lower bounded by the inverse of α modulo $p - 1$, a quantity which in practice corresponds to a dense integer of $\mathbb{Z}/(p-1)\mathbb{Z}$. We deduce that one call to the open $\texttt{Flystel}_\texttt{p}$ is likely to be of maximum degree and is therefore sufficient to thwart attacks that exploit the low degree of a component, such as higher order differentials.

4.5 Implementation Aspects

For direct computation, (or witness calculation) one can simply implement the open `Flystel`. For the verification however, we also have the option to use the closed `Flystel` structure, since there is no requirement for the various verification steps to be performed in a particular order as long as consistency is enforced. In this case, the cost is one multiplication for Q_γ and Q_δ, and as many as are needed to compute $x \mapsto x^\alpha$. This can be implemented using a technique slightly more subtle than basic fast exponentiation, instead relying on addition chains as discussed for example in [BC90]. Good addition chains can be found using the `addChain` tool [McL21]. They are also particularly useful for implementing $x \mapsto x^{1/\alpha}$.

5 Description of `Anemoi`

In this section, we present new primitives, and the way to deterministically construct all of their variants. At their core are the `Anemoi` permutations, that operate on $\mathbb{F}_q^{2\ell}$ for any field size q that is either a prime number or a power of two, and for positive integer ℓ. The round function of these permutations is presented in Section 5.1: for each value of ℓ, and for each value of q, there is a unique round function.

In order to build the primitives themselves, we need also to consider the security level required as it will influence the number of rounds of the permutation (note that the security level will also influence the size of the internal state). The procedures to follow to define higher level algorithms are described in Section 5.2. We then provide some specific instances in Section 5.3.

5.1 Round Function

A round function is a permutation of $\mathbb{F}_q^{2\ell}$, where $\ell > 0$ is an integer, and where q is either[4] a prime number or a power of 2 with a bitlength of at least 10.

In order to define it, we organize its state into a rectangle of elements of $\mathbb{F}_q$ of dimension $2 \times \ell$. The elements in the first row are denoted $(x_0, ..., x_{\ell-1})$, and those in the second row are $(y_0, ..., y_{\ell-1})$ (see Figure 5a). We refer to vectors of $\mathbb{F}_q^{\ell}$ using the same upper-case letters, e.g. $(x_0, ..., x_{\ell-1})$ is denoted X. Subscripts correspond to indices within a vector of $\mathbb{F}_q^{\ell}$, and superscripts to round indices, so X^i is the top part of the state at the start of round i. We let g be a specific generator of the multiplicative subgroup of the field $\mathbb{F}_q$. If q is prime, then g is the smallest such generator using the usual integer ordering. Otherwise, we have that $\mathbb{F}_q = \mathbb{F}_{2^n} = \mathbb{F}_2[x]/p(x)$, where p is an irreducible polynomial of degree n, in which case we let g be one of its roots.

The function applied during round r is denoted R_r. It has a classical Substitution-Permutation Network structure, whose components are described below: first the linear layer, then the S-box layer, and finally the constant addition. The overall action of each of these operations on the state is summarized in Figure 5, and a complete round is represented in Figure 6.

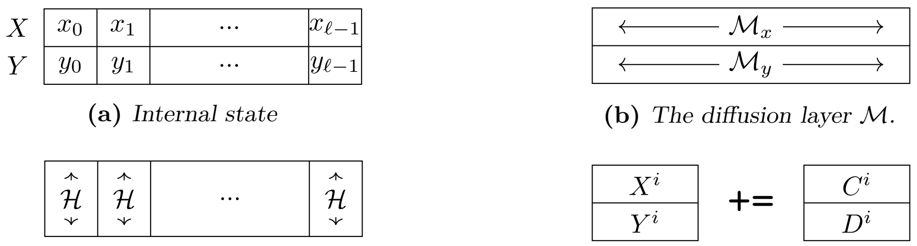

(a) *Internal state* **(b)** *The diffusion layer $\mathcal{M}$.*

(c) *The S-box layer $\mathcal{S}$.* **(d)** *The constant addition $\mathcal{A}$.*

Figure 5: *The internal state of* `Anemoi` *and its basic operations.*

Diffusion Layer $\mathcal{M}$. If $\ell > 1$, then the diffusion layer $\mathcal{M}$ operates on X and Y separately, so that

$$\mathcal{M}(X, Y) = \big(\mathcal{M}_x(X), \mathcal{M}_y(Y)\big) ,$$

as summarized in Figure 5b. The linear permutations $\mathcal{M}_x$ and $\mathcal{M}_y$ are closely related, but differ in order to break the column structure imposed by the non-linear layer (see below). More precisely, we impose that $\mathcal{M}_x$ is a matrix of size $\ell \times \ell$ of $\mathbb{F}_q$ with maximum diffusion, i.e. such that its branching number[5] is equal to $\ell + 1$. We then construct $\mathcal{M}_y$ as $\mathcal{M}_y = \mathcal{M}_x \circ \rho$, where ρ is a simple word permutation: $\rho(x_0, ..., x_{\ell-1}) = (x_1, ..., x_{\ell-1}, x_0)$.

The specifics of the linear permutation $\mathcal{M}_x$ then depend on the value of ℓ. Furthermore, in order for our permutation to best satisfy different proof systems, we use different techniques to construct them. At a high level, there are two different situations:

[4] The field order must have a bitlength of at least 10 bits. The aim of this restriction is to ensure that e.g. MDS matrices can be found as those might not be defined for small field sizes.

[5] Recall that the branching number of a linear permutation L is the minimum over $x \neq 0$ of $\mathrm{hw}(x) + \mathrm{hw}(L(x))$, where hw counts the number of non-zero elements.

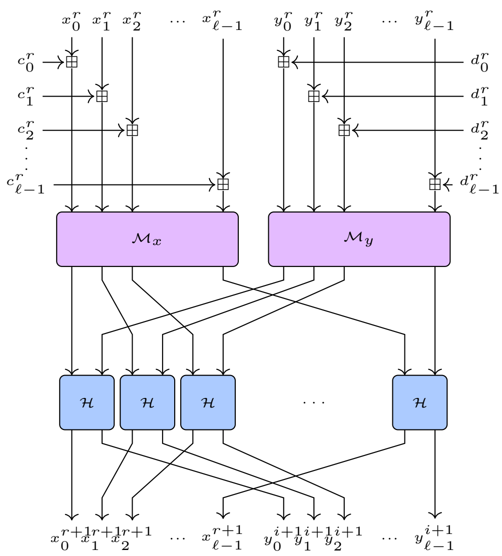

(a) *(Assuming ℓ >1)*

▷ Constant addition
for $i \in \{0, ..., \ell-1\}$ **do**
  $x_i \leftarrow x_i + c_i^r$
  $y_i \leftarrow y_i + d_i^r$
end for
▷ Linear layer $\mathcal{M}$
if $\ell > 1$ **then**
  $X \leftarrow \mathcal{M}_x(X)$
  $Y \leftarrow \mathcal{M}_x \circ \rho(Y)$
else
  $(x_0, y_0) \leftarrow \mathcal{M}_x(x_0, y_0)$
end if
▷ S-box layer $\mathcal{H}$
for $i \in \{0, ..., \ell-1\}$ **do**
  $x_i \leftarrow x_i - gQ(y_i)$
  $y_i \leftarrow y_i - x_i^{1/\alpha}$
  $x_i \leftarrow x_i + gQ(y_i) + g^{-1}$
end for
return (X, Y)

(b)

Figure 6: R_r, *the r-th round of* `Anemoi`*, applied on the state* $(X, Y) \in \mathbb{F}_q^\ell \times \mathbb{F}_q^\ell$*, where* $X = (x_0, ..., x_{\ell-1})$ *and* $Y = (y_0, ..., y_{\ell-1})$*.*

- if ℓ is small, then the value of the field size is expected to be large in order for the permutation to operate on a state large enough to offer security against generic attacks, meaning that this case is expected to happen when using pairing-based proof systems like Groth16 or standard Plonk which require large scalar fields for security.
- if ℓ is large, then the situation is the opposite, meaning that we would expect the field size to be smaller and thus to correspond to e.g. in FRI-based proving systems.

In the Plonk case, additions have a non-negligible cost during verification. As a consequence, when ℓ is at most equal to 4, we use linear layers requiring a number of additions as small as possible. To this end, we adapt results from [DL18] where Duval and Leurent present generic matrix constructions with a minimal number of additions. In practice, when $\ell \in \{1, 2, 3, 4\}$, we use the matrix $\mathcal{M}_x^\ell$ where

$$\mathcal{M}_x^1 = \mathcal{M}_x^2 = \begin{bmatrix} 1 & g \\ g & g^2+1 \end{bmatrix}, \mathcal{M}_x^3 = \begin{bmatrix} g+1 & 1 & g+1 \\ 1 & 1 & g \\ g & 1 & 1 \end{bmatrix}, \mathcal{M}_x^4 = \begin{bmatrix} 1 & 1+g & g & g \\ g^2 & g+g^2 & 1+g & 1+2g \\ g^2 & g^2 & 1 & 1+g \\ 1+g & 1+2g & g & 1+g \end{bmatrix}.$$

If $\ell = 1$, then there is a unique column in the internal state. In this case, to destroy some undesirable patterns at the S-box level, we still use a linear layer, except that it is applied on the vector (x_0, y_0).

Low-addition implementations are shown in Appendix C, and the corresponding diagrams are given in Figure 7. As [DL18] contains several different matrices for each number of inputs, we based our matrices on their candidates that have the lowest number of additions, and the least symmetries.

In the AIR (STARK) case, linear operations are essentially free. Thus, the dominating constraint on a linear layer is its native implementation cost, i.e. the time it takes for a C or Rust program to evaluate $\mathcal{M}_x(x)$. To minimize this cost, we need to minimize the value of the coefficients appearing in the matrix. To this end, we use the circulant matrix where the first row is the smallest in the lexicographic order, and such that the overall matrix is MDS. A script implementing this generation method is provided in Appendix C.

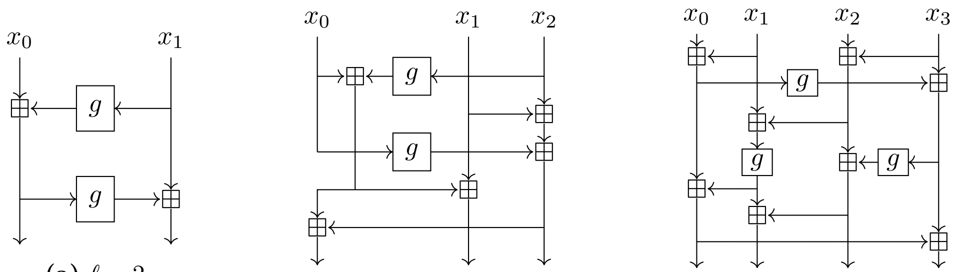

(a) $\ell = 2$. **(b)** $\ell = 3$. **(c)** $\ell = 4$.

Figure 7: *Diagram representations of* $\mathcal{M}_x$.

S-box Layer $\mathcal{S}$. Let $\mathcal{H}$ be an open Flystel operating over $\mathbb{F}_q^2$. Then we let

$$\mathcal{S}(X, Y) = \left(\mathcal{H}(x_0, y_0), ..., \mathcal{H}(x_{\ell-1}, y_{\ell-1})\right) ,$$

as summarized in Figure 5c. A Flystel instance is defined by 4 parameters, regardless of whether it is a $\texttt{Flystel}_\texttt{p}$ or $\texttt{Flystel}_2$: the exponent α, the multiplier β, and the two added constants γ and δ. First, we let $\beta = g$: setting $\beta = 1$ would lead to the invariant space (Section A.3) having equation (x^2, x), which we deem too simple; g is then the most natural non-trivial constant. Furthermore, in order to break the symmetry of the Flystel, we impose that $\gamma \neq \delta$. We thus let $\gamma = 0$ and $\delta = g^{-1}$ as this value is both different from 1 and g while retaining a simple definition.

All that remains is to choose the exponent α. If $q = 2^n$, then we let $\alpha = 3$: we have to use a Gold exponent (i.e. of the shape $2^k + 1$), and 3 always works since n is odd. Otherwise, when q is prime, the process is a bit more involved as a higher value allows using fewer rounds to thwart Gröbner-basis-based attacks, but is also more expensive. Users should use the value of α that yields the most efficient algorithm according to their metrics.

Constant Additions $\mathcal{A}$. We let $x_j \leftarrow x_j + c_j^i$ and $y_j \leftarrow y_j + d_j^i$, where $c_j^i \in \mathbb{F}_q$ and $d_j^i \in \mathbb{F}_q$ are round constants that depend on both the position (index j) and the round (index i). The aim is to increase the complexity of the algebraic expression of multiple rounds of the primitive and to prevent the appearance of patterns that an attacker could leverage in their attack.

They are derived using the digits of π using the following procedure. We let

$$\begin{aligned}&(\pi_0, \pi_1) = \\ &(1415926535897932384626433832795028841971693993751058209749445923078164062862089986280348253421170679, \\ &8214808651328230664709384460955058223172535940812848111745028410270193852110555964462294895493038196)\end{aligned}$$

be the first and second blocks of 100 digits of π. We derive the round constants c_j^i and d_j^i by applying an open Flystel with the same parameters as in the round function on the pair (π_0^i, π_1^j), where superscripts are exponents, so that

$$\begin{cases} c_j^i &= g(\pi_0^i)^2 + \left(\pi_0^i + \pi_1^j\right)^\alpha \\ d_j^i &= g(\pi_1^j)^2 + \left(\pi_0^i + \pi_1^j\right)^\alpha + g^{-1} \end{cases} ,$$

where the computations are done in $\mathbb{F}_q$. When $q = 2^n$, π_0 and π_1 are cast to field elements using the usual mapping sending $\sum_{k=0}^{n-1} x_i 2^i$ to $\sum_{k=0}^{n-1} x_i g^i$, where $(x_0, ..., x_{n-1})$ is the binary representation of x modulo 2^n.

5.2 Higher Level Algorithms

`Anemoi`. The `Anemoi` permutation iterates n_r rounds of the round function described in Figure 6, followed by a call to the linear layer $\mathcal{M}$:

$$\texttt{Anemoi}_{q,\alpha,\ell} \;=\; \mathcal{M} \circ \mathsf{R}_{n_r-1} \circ \ldots \circ \mathsf{R}_0 \; .$$

In symmetric cryptography, we usually *remove* outer linear layers, e.g. in the AES. That is because they don't contribute to the cryptographic strength of a block cipher (e.g. can be removed "for free" by an adversary). In the case of a sponge construction however, the adversary only controls a part of the state, namely the outer part (the rate). Thus, starting/finishing with a diffusion layer ensures that this control is spread across the full state in a way which is not aligned with the non-linear layer. A similar goal could be achieved using *indirect injection*, as is done in Esch [BBC+20].

The number of rounds n_r is computed using the following rule that is derived from our security analysis in Section 6. Let s be the required security level, and (q, ℓ, α) be the parameters imposed by the use case. As we believe that a construction with more branches gives more freedom to the attacker, we choose a security margin that increases with the size of the internal state. Then the number of rounds n_r is the smallest value satisfying both of the following conditions:

$$\begin{aligned} n_r &\geq 10, \text{ and} \\ n_r &\geq \underbrace{1+\ell}_{\text{security margin}} + \underbrace{\min\left\{ r \in \mathbb{N} \;\middle|\; \binom{2\ell r + \alpha + 1 + 2\cdot(\ell r - 2)}{2\ell r}^2 \geq 2^s \right\}}_{\text{to prevent algebraic attacks, see Section 6.2}} . \end{aligned} \quad (2)$$

We derived the number of rounds needed for various values of ℓ and α. They are in Appendix A.4.

`AnemoiSponge`. This function is a "regular" hash function, in the sense that it should be able to process messages of arbitrary length. We therefore rely on the sponge construction detailed in Section 3, where r words are used as the rate, c are used as the capacity, and where the permutation is the `Anemoi` instance operating on $\mathbb{F}_q^{r+c}$. Note that the inner workings of `Anemoi` imply that $r + c$ must be even.

`AnemoiJive`. We can construct a compression function mapping b-to-1 vectors of $\mathbb{F}_q^m$ elements, using Jive_b and an `Anemoi` instance operating on bm elements of $\mathbb{F}_q$. The only constraint is, again, that bm must be even.

Security Claims. All the `Anemoi` permutations generated as defined above can be used safely to construct cryptographic primitives with the given security level. In particular, we make a "hermetic sponge" claim about all the hash functions `AnemoiSponge` generated as above, and we claim that all the `AnemoiJive` functions are secure b-to-1 compression functions (provided of course that the state size is chosen correctly).

5.3 Specific Instances

In this section, we present some examples of functions in the `Anemoi` family that are defined over different fields, aim for different APIs (both `AnemoiSponge` and `AnemoiJive`), and for a security level of 127 bits.

We consider the case of the BLS12-381 curve, in which case $(\log_2(q), \alpha, g) = (255, 5, 7)$, and the case of the BN-254 curve, in which case $(\log_2(q), \alpha, g) = (254, 5, 2)$. In both cases, we aim for 127 bits of security.

AnemoiJive. AnemoiJive-BLS12-381 and AnemoiJive-BN-254 are Merkle Compression functions mapping two elements of $\mathbb{F}_q$ to a unique one. In order to reach a security level of 127 bits, $\ell = 1$ is sufficient in both cases. The underlying permutations of the compression functions then use the following components.

S-box. $\mathcal{H}$ uses the parameters g and α corresponding to the elliptic curve.

Linear layer. As $\ell = 1 < 4$, we use the corresponding low-addition linear layers $\mathcal{M}_x$. For BLS12-381 and BN-254, these are respectively

$$\mathcal{M}_x^{\text{BLS12-381}} = \begin{bmatrix} 1 & 7 \\ 7 & 50 \end{bmatrix} \quad \text{and} \quad \mathcal{M}_x^{\text{BN-254}} = \begin{bmatrix} 1 & 5 \\ 5 & 26 \end{bmatrix} . \tag{3}$$

Round Constants. These are generated as described in Section 5.1.

Number of Rounds. Using Equation (2), we obtain that 19 rounds are needed for a security level of 127 bits.

Round r is then defined as $\mathsf{R}_r : (x, y) \mapsto \mathcal{H} \circ \mathcal{M}(x + c_r, y + d_r)$, and we define the compression functions as follows. Let (x, y) be the input, and P be the Anemoi instance defined by $P := \mathcal{M} \circ \mathsf{R}_{18} \circ ... \circ \mathsf{R}_0$. Then AnemoiJive$(x, y)$ is evaluated as follows: first, let $(u, v) \leftarrow P(x, y)$, then, return $x + y + u + v$.

Security Claims. The best way to find collisions in AnemoiJive-BLS12-381 (respectively AnemoiJive-BN-254) is to rely on a generic collision search. Since the output is an element of $\mathbb{F}_q$ with $\log_2(q) \geq 254$, this is expected to require about 2^{127} function calls on average.

AnemoiSponge. AnemoiSponge-BLS12-381 and AnemoiSponge-BN-254 are hash functions mapping a sequence $\{x_i\}_{0 \leq i < m}$ of elements of $\mathbb{F}_q$ to an element of $\mathbb{F}_q$, where m is a positive integer. It is constructed using a sponge which relies on Anemoi as the permutation. We aim to provide about 127 bits of security, meaning that a capacity of 1 word of $\mathbb{F}_q$ is enough in both cases. We then pick an identical rate, so that $r = c = 1$, and thus $\ell = 1$. The permutations used are then the same as for AnemoiJive-BLS12-381 and AnemoiJive-BN-254.

Security Claims. We claim that AnemoiSponge-BLS12-381 and AnemoiSponge-BN254 provide 127 bits of security against all known attacks.

6 Security Analysis

The security of our high level algorithms is reduced to the security of their inner permutation, namely the Anemoi family. In this section, we argue that the latter has sufficient security level.

6.1 "Classical" Attacks

We call "classical" attacks those that have been used to target algorithms designed over $(\mathbb{F}_2)^n$. As we argue below, we do not expect those to be a significant problem. More detailed arguments are provided in Appendix A.

Statistical attacks like differential and linear cryptanalysis exploit patterns that exist at the S-box level, and which are then propagated through the linear layers to form so-called "trails". As the Flystel has excellent differential and linear properties, we do not expect those to pose a threat (especially given that our linear layers are MDS).

For integral attacks and invariant subspaces, we rely on the fact that our round structure is not "aligned", meaning that the non-linear and linear layers operate over different alphabets (the columns and the rows). As a consequence, the propagation of the patterns exploited by these attacks is hindered. Similarly, thanks to the MDS matrix, truncated differentials, boomerang attacks and MitM attacks also do not pose a threat.

We refer the reader to Appendix A for a more detailed security analysis of the proposed constructions with respect to classical attacks.

6.2 Algebraic Attacks

In this section, we evaluate the security of `Anemoi` with respect to Gröbner basis attacks. As we are mainly interested in a minimal condition on the number of rounds to reach a security of 2^s bits, we allow ourselves to *underestimate* complexity in several places, out of caution. For practical reasons, we restrict our experiments to $\ell = 1$ for even and odd characteristics. We focus on the following version of the CICO (Constrained Input Constrained Output) problem:

Definition 3. Let $P : \mathbb{F}_q^2 \to \mathbb{F}_q^2$ be a permutation. The CICO problem consists in finding $(y_{\text{in}}, y_{\text{out}}) \in \mathbb{F}_q^2$ such that $P(0, y_{\text{in}}) = (0, y_{\text{out}})$.

Solving method.

There are plenty of ways to model CICO as an algebraic system. In this paper, we consider the possibly most promising one for `Anemoi` which is by introducing equations and variables at each round. Such an approach was already proposed to study similar arithmetization-oriented primitives [DGGK21, BSGL20, GØSW22]. More precisely, for $0 \le j \le n_r - 1$, we define f_j and g_j by

$$(x_{j+1}, y_{j+1}) = \mathsf{R}_j(x_j, y_j) \Leftrightarrow \begin{cases} f_j := f(x_j, y_j, x_{j+1}, y_{j+1}) & = 0 \\ g_j := g(x_j, y_j, x_{j+1}, y_{j+1}) & = 0, \end{cases}$$

where R_j is the round function and where f and g are closely related to the verification equations. Also, let $\mathcal{F} := \{f_0, g_0, f_1, g_1, \ldots, f_{n_r-1}, g_{n_r-1}\}$ and let $\mathcal{F}_{\mathsf{CICO}} := \mathcal{F} \cup \{x_0, x_{n_r}\}$. This system contains $2n_r$ equations and $2n_r$ variables. To solve it, we apply the standard *zero-dimensional* strategy:

1. Compute a Gröbner basis $\mathcal{G}_{\text{drl}}$ for a DRL ordering [Lou94, Definition 1.4.3],
2. Compute a new Gröbner basis $\mathcal{G}_{\text{lex}}$ for the LEX ordering by using the FGLM algorithm [FGLM93] on $\mathcal{G}_{\text{drl}}$.

For Step 1, the running time of Gröbner basis algorithms such as F4 [Fau99] or F5 [Fau02] is usually estimated by evaluating the *solving degree* of the system denoted by d_{solv}. This degree can be informally defined as the maximal degree of a polynomial which occurs during the Gröbner basis computation. Once d_{solv} is known, a generic estimate for the cost of F4/F5 is

$$\mathcal{O}\left(\binom{d_{\text{solv}} + n_v}{n_v}^{\omega}\right) \tag{4}$$

field operations, where n_v is our number of variables and where $2 \le \omega \le 3$ is a linear algebra constant. We stress that this estimation is heuristic and it is an upper bound that does not take into account the structure or the sparsity of the given Macaulay matrices. In particular, to use it as a guidance, we will adopt the conservative $\omega = 2$ for the linear algebra constant. Also, contary to other arithmetization-oriented primitives (see for instance [BSGL20]), we notice that Step 2 had a negligible cost compared to Step 1. Due to space constraints, details on the complexity of this FGLM step are presented in Appendix B.3 and we now estimate $d_{\text{solv}}(I_{\mathsf{CICO}})$ for Anemoi when $\ell = 1$.

6.2.1 Characteristic 2.

When $q = 2^n$ for odd n, recall that $\alpha = 3$, $Q_i(x) = \beta x^3 + \gamma$ and $Q_f(x) = \beta x^3 + \delta$. The $\mathcal{F}_{\mathsf{CICO}}$ system then contains $2n_r$ cubic polynomials in $2(n_r + 1) - 2 = 2n_r$ variables. For such a system, one usually relies on the Macaulay bound for an upper bound on d_{solv}, namely $2n_r(3-1)+1 = 4n_r + 1$. This bound would be tight if the system of homogeneous parts of highest degree was *regular*. However, our experiments indicate that $\mathcal{F}_{\mathsf{CICO}}$ does not behave as such, see Appendix B.1. Therefore, we chose to extrapolate these data to find a lower bound on d_{solv}. As this method might lead to inaccuracies for a higher number of rounds, our bound is voluntarily very coarse.

Conjecture 1. *For $n_r \geq 2$, the maximal degree $d_{solv}(I_{\mathsf{CICO}})$ which occurs while computing a* DRL-*Gröbner basis for I_{CICO} is such that $d_{solv}(I_{\mathsf{CICO}}) \geq 3n_r$.*

Finally, we evaluate the complexity of Step 1 using Equation (4) with the lower bound on $d_{\text{solv}}(I_{\mathsf{CICO}})$ given by Conjecture 1 and $n_v = 2n_r$.

6.2.2 Odd characteristic.

When $q > 2$ is an odd prime, the equations f_j and g_j are affine of degree α but it has already been noted in the proof of Proposition 3 that their difference $h_j := f_j - g_j$ is a quadratic polynomial. In particular, taking $\{f_j, h_j\}$ instead of $\{f_j, g_j\}$ as a generating set for each round does not change the final ideal I_{CICO} but it better captures the specificity of the system. In contrast to the even characteristic case, an important remark is that the equations have a part of degree 2 due to the expressions of Q_i and Q_j and a degree α part due to the $x \mapsto x^\alpha$ permutation. This feature seems to make the analysis of d_{solv} slightly more complicated, for instance it is not encompassed in a standard Hilbert series which is a common tool to estimate d_{solv}. Experimentally, the behaviour of $\mathcal{F}_{\mathsf{CICO}}$ was clearly not the one of a generic system especially when α grows. Our experiments as well as further explanations are provided in Appendix B.2, and from them we also propose

Conjecture 2. *For $n_r \geq 2$, the maximal degree $d_{solv}(I_{\mathsf{CICO}})$ which occurs while computing a* DRL-*Gröbner basis for I_{CICO} is such that $d_{solv}(I_{\mathsf{CICO}}) \geq \alpha + 1 + 2(n_r - 2)$.*

From Conjecture 2 we can then derive a lower bound for the cost of Step 1 in the same way as in even characteristic.

Several columns.

When $\ell > 1$, the number of equations and variables is naturally multiplied by ℓ and thus experiments were extremely difficult to conduct. We generalize our formulae to $\ell > 1$ by replacing n_r by $\ell \cdot n_r$ everywhere, which is natural when looking at the expressions of the Macaulay bound. Similarly, we note that the bounds given for Rescue in [BSGL20] exhibit this extra ℓ factor.

7 Benchmarks

In this section, we compare various instances of Rescue–Prime, Poseidon, Griffin and Anemoi with respect to SNARK metrics: R1CS (Section 7.1) and Plonk (Section 7.2), and STARK: AIR (Section 7.3). For Plonk performance, we will also conduct a comparison with Reinforced Concrete.

Due to the increasing number of projects revolving around zk-STARKs, which do not require an algebraic group with large underlying fields, we also illustrate native performance comparison of 2-to-1 compression functions based on *Rescue'*, Poseidon and Anemoi on a 64-bit field used in various projects ([add22], [Zer22]).

To do so, we need to set the parameters. Then, let $\mathbb{F}_q$, where $q = p$, be a prime field, and let m be the number of field elements we operate on ($m = 2\ell$ for `Anemoi`). Besides, let s denote the security level in bits, n_r the number of rounds, and $\mathcal{C}_\alpha$ the cost of an exponentiation $x \mapsto x^\alpha$.

Rescue–Prime requires $1.5 \cdot \max\{5, \lceil (s+2)/4m \rceil\}$ rounds when $\alpha = 3$ and $1.5 \cdot \max\{5, \lceil (s+3)/5.5m \rceil\}$ rounds when $\alpha = 5$ (see [AAB+20, SAD20]). Poseidon has $n_r = \mathsf{RF} + \mathsf{RP}$ rounds. While the bound is a complex expression, in our setting and for the safety margin recommended by the authors, it holds that $\mathsf{RF} = 8$, and that RP must be higher than (or equal to) $1.075 \cdot (\lceil \log_\alpha(2) \cdot \min\{s, \log_2(p)\} \rceil + \lceil \log_a m \rceil - \mathsf{RF})$. Griffin requires at least $\lceil 1.2 \max\{6, 1 + R_{\mathsf{GB}}\} \rceil$ rounds where R_{GB} is the smallest integer such that $\min\left\{ \binom{R_{\mathsf{GB}} \cdot (\alpha+m)+1}{1+m \cdot R_{\mathsf{GB}}}, \binom{\alpha^{R_{\mathsf{GB}}}+1+R_{\mathsf{GB}}}{1+R_{\mathsf{GB}}} \right\} \geq 2^{s/2}$.

While we also consider $\alpha = 17$ as a good exponent (the cost of an exponentiation for $\alpha = 17$ is not so far from an exponentiation for $\alpha = 5$), we will compare here only instances with $\alpha = 3$ and $\alpha = 5$, as previously proposed in the other designs. In the following, we use the n_r values from Section 5.2. Concrete values are presented in Appendix A.4.

7.1 R1CS Systems

We first estimate the number of constraints for R1CS. Using the *closed* ***`Flystel`*** of Figure 3b, we obtain the following verification equations for the S-Box:

$$\begin{cases} (v-y)^\alpha + \beta y^2 + \gamma - x = 0 \\ (v-y)^\alpha + \beta v^2 + \delta - u = 0 \ . \end{cases} \tag{5}$$

Then, evaluating one S-Box costs $\mathcal{C}_\alpha$ constraints to obtain $(v-y)^\alpha$, and 1 constraint for each of the two quadratics. For Rescue–Prime and Poseidon, each S-Box costs $\mathcal{C}_\alpha$ constraints. For Griffin, each S-Box costs $2 \cdot \mathcal{C}_\alpha$ constraints for the first two words, and 1 constraint for each squaring of L and each word of the remaining state. As a consequence, when using Rescue–Prime, Poseidon, Griffin and `Anemoi` as hash functions in sponge mode, the number of constraints is respectively $\mathcal{C}_\alpha \cdot 2m \cdot n_r$, $\mathcal{C}_\alpha \cdot (m\mathsf{RF} + \mathsf{RP})$, $(\mathcal{C}_\alpha + m - 2) \cdot 2n_r$ and $(\mathcal{C}_\alpha + 2) \cdot (\frac{m}{2} \cdot n_r)$.

We compare the number of constraints for those four schemes in Table 1. As we can see, the `Anemoi` permutations are consistently much more efficient than both Poseidon and Rescue–Prime by about a factor 2. Besides `Anemoi` and Griffin are on par, and `Anemoi` takes the advantage for $\alpha = 3$.

7.2 Plonk

For ease of exposition, we will consider rounds to be shifted so that constant additions and linear operations come after the S-box. As for R1CS, we again investigate Equation (5). In standard Plonk, evaluating an S-Box costs 1 constraint to derive $w = y - v$ and $\mathcal{C}_\alpha$ constraints to obtain w^α, 1 constraint for each of the two quadratics, and 1 each for the sums on x, u. The total cost for the S-box layer with 3 wires is $(\mathcal{C}_\alpha + 5)\frac{m}{2}$.

The constant additions can be folded into the $n_r + 1$ linear layers and can thus be disregarded. For $m > 2$, the linear layer itself consists of 2 separate matrix-vector multiplications, each producing $\frac{m}{2}$ sums of $\frac{m}{2}$ terms, requiring $m \cdot (\frac{m}{2} - 1)$ constraints. However, the number of constraints per matrix multiplication can be lowered by choosing MDS matrices lowering the number of additions. For the matrices given for $m = 6$ and $m = 8$ in 5.1, we have respectively a cost of 10 and 16 per linear layer. For $m = 2$, the linear layer is different, and we only require 2 constraints, which is especially relevant for the Jive_2 mode of operation.

Poseidon uses simpler S-Boxes, each costing $\mathcal{C}_\alpha$ constraints. Full rounds use m S-boxes whereas partial ones use only one. The linear layer costs $m \cdot (m - 1)$ constraints for all

Table 1: *Total R1CS, Plonk and AIR cost for several hash functions ($s = 128$).*

(a) *when $\alpha = 3$.*

	m	*Rescue'*	POSEIDON	GRIFFIN	Anemoi
R1CS	2	208	198	-	**76**
	3	216	214	**96**	-
	4	224	232	112	**96**
	6	216	264	-	**120**
	8	256	296	176	**160**
Plonk	2	312	380	-	**173**
	3	432	760	**197**	-
	4	560	1336	291	**220**
	6	756	3024	-	**320**
	8	1152	5448	635	**456**
AIR	2	156	300	-	**114**
	3	162	324	**144**	-
	4	168	348	168	**144**
	6	**162**	396	-	180
	8	**192**	480	264	240

(b) *when $\alpha = 5$.*

	m	*Rescue'*	POSEIDON	GRIFFIN	Anemoi
R1CS	2	240	216	-	**95**
	3	252	240	**96**	-
	4	264	264	**110**	120
	6	288	315	-	**150**
	8	384	363	**162**	200
Plonk	2	320	344	-	**192**
	3	420	624	**173**	-
	4	528	1032	253	**244**
	6	768	2265	-	**350**
	8	1280	4003	543	**496**
AIR	2	200	360	-	**190**
	3	210	405	**180**	-
	4	**220**	440	**220**	240
	6	**240**	540	-	300
	8	**320**	640	360	400

rounds. Rescue–Prime uses m standard and m inverted S-Boxes, each costing $\mathcal{C}_\alpha$. Each round also utilizes 2 independent linear layers each costing $m \cdot (m-1)$ constraints for all rounds.

For GRIFFIN, the cost of the S-BOX is $2 \cdot C_\alpha + 3 + 4 \cdot (m-3)$. Regarding the linear layer, the circulant matrix $Circ(2,1,1)$ used for $m = 3$ can be computed in 5 constraints. For $m = 4$, the cost of one multiplication by the matrix $Circ(3,2,1,1)$ is 11. By observing intermediate variables from the S-BOX computation can be reused in the linear layer computation, Griffin gives 253 constraints for $m = 4$ (resp. 543 for $m = 8$).

We then compare the number of constraints for these four schemes in Table 1. Again, Anemoi is consistently ahead of the competition with a significant margin.

7.2.1 Plonk Optimizations.

One of the more fruitful, but also challenging aspects of Plonk is its ability to extend the expressive power of the constraints at a reasonable cost. In the analysis, the linear layer cost dominates that of the S-Boxes. This is particularly impactful for POSEIDON, as the efficiency benefit of its partial rounds is negated. The recent work of Ambrona et al. [ASTW22] presents a set of generic and tailored optimizations for Plonk applicable to POSEIDON.

While an exhaustive comparison of optimization options is beyond the scope of this work, real-world usage implies that a reasonable set of optimizations have been applied before deployment. For this reason, we perform a minimal comparison between: POSEIDON as optimized by Ambrona et al., and Reinforced Concrete [BGK+21] which was built with Plonk optimizations in mind, and Anemoi. As POSEIDON and Reinforced Concrete are sponge based we use $s = 128, \alpha = 5$ and $m = 3$ to represent popular deployment choices, while we set $m = 2$ for Anemoi, using the Jive_2 mode . For comparison we also extrapolate a Jive_2 versions of POSEIDON with the optimizations of [ASTW22], and Reinforced Concrete.

We use one of the constraint systems used by Ambrona et al. [ASTW22]: a 3-wire constraint system with a x^5, as well as selectors for the next constraint wires:

$$q_L.a + q_R.b + q_O.c + q_M.a.b + q_5.c^5 + q_{L'}.a' + q_{R'}.b' + q_{O'}.c' \ .$$

At a base level, the relations we need to express one $\texttt{AnemoiJive}_2$ round are[6]

[6] For readability, we omit the coefficients for the linear layer.

Table 2: *Constraints comparison of several hash functions for Plonk with an additional custom gate to compute x^5. We fix $s = 128$, and prime field sizes of 256.*

	m	Constraints
Poseidon	3	110
	2	88
Reinforced Concrete	3	378
	2	236
Griffin	3	125
AnemoiJive	2	**79**

(a) *With 3 wires.*

	m	Constraints
Poseidon	3	98
	2	82
Reinforced Concrete	3	267
	2	174
Griffin	3	111
AnemoiJive	2	**58**

(b) *With 4 wires.*

1. $y - v - w = 0$
2. $w^5 + \beta yy + \gamma - x = 0$
3. $w^5 + \beta vv + \delta - u = 0$
4. $\tilde{u} - u - v - \rho = 0$
5. $\tilde{v} - u - v - \kappa = 0$

where $\tilde{u}, \tilde{v}$ are the values of u, v after the linear layer and ρ, κ are derived from round constants. We can save one constraint by calculating $\tilde{u}$ directly and eliminating u. We also need to make sure that the relations fit into the available wires, and make sure that the last constraint leaves the "next constraint" wires free, so that each set of round constraints can be followed by any constraint without restriction. To accomplish this, we also need to perform some reordering. Setting $\rho' = \rho + \delta$, the end result is:

1. $w^5 + \beta yy + \gamma - x = 0,$ where: $(a, b, c) = (y, y, w)$ and $(a', b',' c') = (x\_, \_)$,
2. $y - v - w = 0,$ where: $(a, b, c) = (x, y, w)$ and $(a', b',' c') = (v, \_, \_)$,
3. $w^5 + \beta vv + \rho' + v - \tilde{u} = 0,$ where: $(a, b, c) = (v, v, w)$ and $(a', b',' c') = (\tilde{u}, \_, \_)$,
4. $\tilde{v} - \tilde{u} - v - \kappa = 0,$ where: $(a, b, c) = (\tilde{u}, \tilde{v}, v)$ and $(a', b',' c') = (\_, \_, \_)$.

Thus, we are able to perform one `AnemoiJive` round in 4 constraints, 2 additional constraints to account for the initial linear layer, and 1 more for the final Jive_2 addition (using the "next" wires). With four wires, we can eliminate w, by having a 5th power gate operate on $y - v$. Rounds are reduced to 3 constraints, and we need only 1 extra constraint for the first linear layer as handle x_0 inline.

We summarize our findings in Table 2. We extrapolate the $m = 2$ costs for Poseidon and `Reinforced Concrete` by assuming a Jive_2 mode of operation is feasible at no additional overhead or increase in rounds. We note while that the costs between Poseidon, `Anemoi` and Griffin are directly comparable as they use the same features (namely x^5 and "next constraint" selectors), `Reinforced Concrete` leverages lookup tables [BGK+21, GW20] instead. We do note that by [ASTW22, Table 2], the additional cost (compared to standard Plonk) for the custom gates we describe is between 10% and 40%.

7.2.2 Plonk optimisations with an additional quadratic custom gate

We can go further in the optimisation given above by extending Plonk with a custom gate to compute the square of a wire, which adds a negligeable overhead to the prover and the verifier time. In the 3-wires setting, having the quadratic custom gate on the wire b frees a wire in the constraints given above and allow us to compute two rounds in 5 constraints as described below [7], giving a total number of constraints of 51.

[7] For readability, the selectors values have been omitted

Table 3: *Native performance comparison of 2-to-1 compression functions for $\mathbb{F}_p$ with $p = 2^{64} - 2^{32} + 1$. We fix $s = 128$. Times are given in μs.*

Rescue–Prime-12-8	Poseidon-12-8	Griffin-12-8	Anemoi-8
11.39	1.93	3.13	3.93

1. $w_0^2 + w_0 y_0 + w_0 - x_0 - y_0 + y_1 + q_c$, where: $(a, b, c) = (y_0, w_0, x_0)$ and $(a', b,' c') = (y_1, \_, \_)$,
2. $w_1^2 + w_1 y_1 - w_0 + w_1 + x_2 + y_0 - y_1 + q_c$, where: $(a, b, c) = (y_1, w_1, w_0)$ and $(a', b,' c') = (y_0, x_2, \_)$,
3. $w_1 - x_2 - y_1 + y_2 - q_c$, where: $(a, b, c) = (y_0, x_2, y_2)$ and $(a', b,' c') = (w_1, y_1, \_)$,
4. $w_1^5 + y_1^2 - w_0 + y_0 - y_1 + q_c$, where: $(a, b, c) = (w_1, y_1, \_)$ and $(a', b,' c') = (w_0, y_0, \_)$.
5. $w_0^5 + y_0^2 - x_0 + q_c$, where: $(a, b, c) = (w_0, y_0, x_0)$ and $(a', b,' c') = (\_, \_, \_)$.

7.3 AIR

Finally, we also study the performance of Anemoi in the Algebraic Intermediate Representation (AIR) arithmetization used in STARKs [BBHR18]. Here, the relevant quantities are: the width of the computation state w, the number of computation steps T, and the maximum degree of the constraints $d_{\max}$. While there are several ways to estimate the cost of a given AIR program given the above quantities, we will consider the total cost to be expressed as $w \cdot T \cdot d_{\max}$, following [AAB+20].

For Rescue–Prime, Griffin and Anemoi, we have $w = m$, $T = n_r$ and $d_{\max} = \alpha$. For Poseidon, we have $w = m$, $T = \mathsf{RF} + \lceil \mathsf{RP}/m \rceil$ and $d_{\max} = \alpha$.

We then compare the total cost for these four schemes in Table 1. Anemoi and Griffin are quite similar, and Anemoi is ahead of Rescue–Prime due to the lower number of rounds for small widths.

7.4 Native performance

Outside of proving systems, Anemoi performance can challenge other algebraic hash functions, especially in a Merkle tree setting thanks to its Jive mode. In particular in STARKs settings where one can use small cryptographic fields, Anemoi offers the best balance in terms of native evaluation and number of constraints. In Table 3, we illustrate the running time of a 2-to-1 compression method with AnemoiJive, Rescue–Prime, Poseidon and Griffin over the 64 bits prime field $\mathbb{F}_p$ with $p = 2^{64} - 2^{32} + 1$. Each instantiation has a 4 field elements (32 bytes) digest size to ensure 128 bits security. Rescue–Prime and Poseidon instantiations both have a state width of 12 elements and rate of 8 elements. Anemoi has a state width of 8 elements[8]. All experiments were performed on an *Intel(R) Core(TM) i7-9750H CPU @ 2.60GHz*. We present average times in microseconds of each experiment running for 5 seconds. Standard deviations are negligible. The mentioned instantiations of Anemoi, Rescue–Prime and Griffin over $\mathbb{F}_p$ are implemented in Rust.

In Table 4, we compare the native performance with Rescue–Prime, Poseidon and Griffin with a state size useful for applications like Merkle tree over the scalar field of

[8] While other instances need to have a sufficiently large rate to absorb two digests with only one permutation call, Anemoi can have any desired rate as it does not come into play in the Jive construction.

Table 4: *Native performance comparison of a permutation for the scalar field of* $BLS12-381$. *We fix* $s = 128$. *Rescue–Prime,* POSEIDON *and* GRIFFIN *are instantiated with a state size of* 3 *and* `Anemoi` *with* $l = 1$. *Times are in* μs.

Rescue–Prime	POSEIDON	GRIFFIN	Anemoi
255.36	14.43	73.66	115.82

BLS12-381. For small state size, the dominant computation for `Anemoi` (like Rescue–Prime and GRIFFIN) is $x^{1/d}$ and requires 305 field operations with an appropriate addition chain taking around $6\mu s$. All experiments were performed on an *Intel(R) Core(TM) i7-8565U CPU @ 1.80GHz*. We present average times in microseconds of each experiment running for 2 seconds. Standard deviations are in the order of tens of nanoseconds. Our implementation uses C via FFI through an OCaml binding, but this introduces a negligible overhead.

8 Conclusion

We have made several contributions towards both the theoretical understanding and the practical use of arithmetization-oriented hash functions. Our main contribution is of course `Anemoi`, a family of permutations that are efficient across various arithmetization methods, yielding gains from 10% up to more than 50% depending on the context, over existing designs. Furthermore, in order to be able to design its main component, the `Flystel` structure, we had to first identify the link between arithmetization-orientation and CCZ-equivalence. We hope that functions such as the `Flystel` itself as well as similar ones will be studied by mathematicians as we believe those to be of independent interest.

Finally, we provided a new simple mode, Jive_b, which adds to the growing list of permutation-based modes of operation providing a b-to-1 compression function, of particular relevance in Merkle trees. It allows us to further improve upon the state-of-the-art, so that `AnemoiJive` requires only 51 Plonk constraints in total (when 3 wires and 2 custom gates are used), compared to the best sponge-based instance of POSEIDON which requires 98 constraints with 4 wires (or 110 with 3) and 1 custom gate. With only one custom gate, `AnemoiJive` requires 58 constraints for 4 wires (or 79 with 3).

Acknowledgements

Thanks to Markulf Kohlweiss, Antoine Rondelet and Duncan Tebbs for proof-reading a draft version of the first version of this paper, and for providing insightful comments and suggestions. Thanks to Duncan Tebbs for providing an independent estimation of the Flystel circuit cost interms of R1CS constraints. The work of Léo Perrin is supported by the European Research Council (ERC, grant agreement no. 101041545 "ReSCALE"). We thank Tomer Ashur for pointing out a mistake in Figure 1. We also thank Miguel Ambrona and Raphaël Toledo for the idea of the quadratic custom gate and their contribution to the Plonk implementation.

References

[AAB+20] Abdelrahaman Aly, Tomer Ashur, Eli Ben-Sasson, Siemen Dhooghe, and Alan Szepieniec. Design of symmetric-key primitives for advanced cryptographic protocols. *IACR Trans. Symm. Cryptol.*, 2020(3):1–45, 2020.

[add22] Polygon miden. Repository https://github.com/maticnetwork/miden, September 2022.

[AGR+16] Martin R. Albrecht, Lorenzo Grassi, Christian Rechberger, Arnab Roy, and Tyge Tiessen. MiMC: Efficient encryption and cryptographic hashing with minimal multiplicative complexity. In Jung Hee Cheon and Tsuyoshi Takagi, editors, *ASIACRYPT 2016, Part I*, volume 10031 of *LNCS*, pages 191–219. Springer, Heidelberg, December 2016.

[ASTW22] Miguel Ambrona, Anne-Laure Schmitt, Raphael R. Toledo, and Danny Willems. New optimization techniques for plonk's arithmetization. Cryptology ePrint Archive, Paper 2022/462, 2022. https://eprint.iacr.org/2022/462.

[Bar04] Magali Bardet. *Étude des systèmes algébriques surdéterminés. Applications aux codes correcteurs et à la cryptographie.* Theses, Université Pierre et Marie Curie - Paris VI, December 2004.

[BBC+20] Christof Beierle, Alex Biryukov, Luan Cardoso dos Santos, Johann Großschädl, Léo Perrin, Aleksei Udovenko, Vesselin Velichkov, and Qingju Wang. Lightweight AEAD and hashing using the Sparkle permutation family. *IACR Trans. Symm. Cryptol.*, 2020(S1):208–261, 2020.

[BBHR18] Eli Ben-Sasson, Iddo Bentov, Yinon Horesh, and Michael Riabzev. Scalable, transparent, and post-quantum secure computational integrity. Cryptology ePrint Archive, Report 2018/046, 2018. https://eprint.iacr.org/2018/046.

[BC90] Jurjen N. Bos and Matthijs J. Coster. Addition chain heuristics. In Gilles Brassard, editor, *CRYPTO'89*, volume 435 of *LNCS*, pages 400–407. Springer, Heidelberg, August 1990.

[BCD+20] Tim Beyne, Anne Canteaut, Itai Dinur, Maria Eichlseder, Gregor Leander, Gaëtan Leurent, María Naya-Plasencia, Léo Perrin, Yu Sasaki, Yosuke Todo, and Friedrich Wiemer. Out of oddity - new cryptanalytic techniques against symmetric primitives optimized for integrity proof systems. In Daniele Micciancio and Thomas Ristenpart, editors, *CRYPTO 2020, Part III*, volume 12172 of *LNCS*, pages 299–328. Springer, Heidelberg, August 2020.

[BCP06] Lilya Budaghyan, Claude Carlet, and Alexander Pott. New classes of almost bent and almost perfect nonlinear polynomials. *IEEE Transactions on Information Theory*, 52(3):1141–1152, 2006.

[BDPA13] Guido Bertoni, Joan Daemen, Michaël Peeters, and Gilles Van Assche. Keccak. In Thomas Johansson and Phong Q. Nguyen, editors, *EUROCRYPT 2013*, volume 7881 of *LNCS*, pages 313–314. Springer, Heidelberg, May 2013.

[BDPVA07] Guido Bertoni, Joan Daemen, Michaël Peeters, and Gilles Van Assche. Sponge functions. In *ECRYPT hash workshop*, number 9. Citeseer, 2007.

[Ber08] Daniel J Bernstein. The Salsa20 family of stream ciphers. In *New stream cipher designs*, pages 84–97. Springer, 2008.

[BGK+21] Mario Barbara, Lorenzo Grassi, Dmitry Khovratovich, Reinhard Lueftenegger, Christian Rechberger, Markus Schofnegger, and Roman Walch. Reinforced concrete: Fast hash function for zero knowledge proofs and verifiable computation. Cryptology ePrint Archive, Report 2021/1038, 2021. https://eprint.iacr.org/2021/1038.

[BS01] Alex Biryukov and Adi Shamir. Structural cryptanalysis of SASAS. In Birgit Pfitzmann, editor, *EUROCRYPT 2001*, volume 2045 of *LNCS*, pages 394–405. Springer, Heidelberg, May 2001.

[BS10] Alex Biryukov and Adi Shamir. Structural cryptanalysis of SASAS. *Journal of Cryptology*, 23(4):505–518, October 2010.

[BSCG+14] Eli Ben-Sasson, Alessandro Chiesa, Christina Garman, Matthew Green, Ian Miers, Eran Tromer, and Madars Virza. Zerocash: Decentralized anonymous payments from bitcoin. Cryptology ePrint Archive, Report 2014/349, 2014. https://ia.cr/2014/349.

[BSGL20] Eli Ben-Sasson, Lior Goldberg, and David Levit. Stark friendly hash – survey and recommendation. Cryptology ePrint Archive, Report 2020/948, 2020. https://ia.cr/2020/948.

[BSV07] Thomas Baignères, Jacques Stern, and Serge Vaudenay. Linear cryptanalysis of non binary ciphers. In Carlisle M. Adams, Ali Miri, and Michael J. Wiener, editors, *SAC 2007*, volume 4876 of *LNCS*, pages 184–211. Springer, Heidelberg, August 2007.

[CCZ98] Claude Carlet, Pascale Charpin, and Victor Zinoviev. Codes, bent functions and permutations suitable for DES-like cryptosystems. *Designs, Codes and Cryptography*, 15(2):125–156, 1998.

[CDP17] A. Canteaut, S. Duval, and L. Perrin. A generalisation of Dillon's APN permutation with the best known differential and nonlinear properties for all fields of size 2^{4k+2}. *IEEE Transactions on Information Theory*, 63(11):7575–7591, Nov 2017.

[CLO07] David Cox, John Little, and Donal O'Shea. Ideals, varieties, and algorithms. an introduction to computational algebraic geometry and commutative algebra. 2007.

[CP19] Anne Canteaut and Léo Perrin. On CCZ-equivalence, extended-affine equivalence, and function twisting. *Finite Fields and Their Applications*, 56:209–246, 2019.

[DGGK21] Christoph Dobraunig, Lorenzo Grassi, Anna Guinet, and Daniël Kuijsters. Ciminion: Symmetric encryption based on toffoli-gates over large finite fields. Springer-Verlag, 2021.

[DL18] Sébastien Duval and Gaëtan Leurent. MDS matrices with lightweight circuits. *IACR Trans. Symm. Cryptol.*, 2018(2):48–78, 2018.

[Dwo15] Morris Dworkin. Sha-3 standard: Permutation-based hash and extendable-output functions, 2015-08-04 2015.

[Fau99] Jean-Charles Faugére. A new efficient algorithm for computing gröbner bases (f4). *Journal of Pure and Applied Algebra*, 139(1):61–88, 1999.

[Fau02] Jean Charles Faugère. A new efficient algorithm for computing gröbner bases without reduction to zero (f5). In *Proceedings of the 2002 International Symposium on Symbolic and Algebraic Computation*, ISSAC '02, pages 75–83, New York, NY, USA, 2002. Association for Computing Machinery.

[FGLM93] J.C. Faugère, P. Gianni, D. Lazard, and T. Mora. Efficient computation of zero-dimensional gröbner bases by change of ordering. *Journal of Symbolic Computation*, 16(4):329–344, 1993.

[FM11] Jean-Charles Faugère and Chenqi Mou. Fast algorithm for change of ordering of zero-dimensional Gröbner bases with sparse multiplication matrices. In *ISSAC 2011 - International Symposium on Symbolic and Algebraic Computation*, pages 115–122, San Jose, United States, June 2011. ACM.

[GHR+22] Lorenzo Grassi, Yonglin Hao, Christian Rechberger, Markus Schofnegger, Roman Walch, and Qingju Wang. A new feistel approach meets fluid-SPN: Griffin for zero-knowledge applications. Cryptology ePrint Archive, Report 2022/403, 2022. https://eprint.iacr.org/2022/403.

[GKR+21] Lorenzo Grassi, Dmitry Khovratovich, Christian Rechberger, Arnab Roy, and Markus Schofnegger. Poseidon: A new hash function for zero-knowledge proof systems. In Michael Bailey and Rachel Greenstadt, editors, *USENIX Security 2021*, pages 519–535. USENIX Association, August 2021.

[GMR89] Shafi Goldwasser, Silvio Micali, and Charles Rackoff. The knowledge complexity of interactive proof systems. *SIAM Journal on Computing*, 18(1):186–208, 1989.

[GØSW22] Lorenzo Grassi, Morten Øygarden, Markus Schofnegger, and Roman Walch. From farfalle to megafono via ciminion: The prf hydra for mpc applications. Cryptology ePrint Archive, Report 2022/342, 2022. https://ia.cr/2022/342.

[Gro16] Jens Groth. On the size of pairing-based non-interactive arguments. In Marc Fischlin and Jean-Sébastien Coron, editors, *EUROCRYPT 2016, Part II*, volume 9666 of *LNCS*, pages 305–326. Springer, Heidelberg, May 2016.

[GW20] Ariel Gabizon and Zachary J. Williamson. plookup: A simplified polynomial protocol for lookup tables. Cryptology ePrint Archive, Report 2020/315, 2020. https://eprint.iacr.org/2020/315.

[Hir16] Shoichi Hirose. Sequential hashing with minimum padding. In *NIST Workshop on Lightweight Cryptography 2016*. National Institute of Standards and Technology (NIST), 2016.

[Knu95] Lars R. Knudsen. Truncated and higher order differentials. In Bart Preneel, editor, *FSE'94*, volume 1008 of *LNCS*, pages 196–211. Springer, Heidelberg, December 1995.

[Lou94] W.W.A.P. Loustaunau. *An Introduction to Grobner Bases*. American Mathematical Soc., 1994.

[LTYW18] Yongqiang Li, Shizhu Tian, Yuyin Yu, and Mingsheng Wang. On the generalization of butterfly structure. *IACR Trans. Symm. Cryptol.*, 2018(1):160–179, 2018.

[McL21] Michael B. McLoughlin. addchain: Cryptographic addition chain generation in go. Repository https://github.com/mmcloughlin/addchain, October 2021.

[Nyb94] Kaisa Nyberg. Differentially uniform mappings for cryptography. In Tor Helleseth, editor, *EUROCRYPT'93*, volume 765 of *LNCS*, pages 55–64. Springer, Heidelberg, May 1994.

[PUB16] Léo Perrin, Aleksei Udovenko, and Alex Biryukov. Cryptanalysis of a theorem: Decomposing the only known solution to the big APN problem. In Matthew Robshaw and Jonathan Katz, editors, *CRYPTO 2016, Part II*, volume 9815 of *LNCS*, pages 93–122. Springer, Heidelberg, August 2016.

[SAD20] Alan Szepieniec, Tomer Ashur, and Siemen Dhooghe. Rescue-prime: a standard specification (SoK). Cryptology ePrint Archive, Report 2020/1143, 2020. https://eprint.iacr.org/2020/1143.

[Zer22] Polygon Zero. Plonky2. Repository https://github.com/mir-protocol/plonky2, September 2022.

Supporting Material

A Details of our Security Analysis

A.1 Differential and Linear Attacks

In this part, we argue that differential and linear attacks can be prevented by the `Flystel` construction, thanks to the differential and linear properties of the scheme as presented in Section 5.

Differential attacks exploit the probability distribution of a given non-zero input difference leading to a given output difference after a certain number of rounds. As established in Proposition 2 for the $\texttt{Flystel}_2$ and in Proposition 3 for the $\texttt{Flystel}_\texttt{p}$, the differential uniformity of a `Flystel` is low (namely 4 in the former case and $(\alpha-1)$ in the latter). As a consequence, the probability of any transition of the form $\mathcal{H}(x+a, y+b) - \mathcal{H}(x,y) = (c,d)$ is small: it is upper bounded by $(\alpha-1)/q^2$. Given that q is typically bigger than 2^{63}, we only need to activate 3 S-boxes to obtain more than 128 bits of security, and 5 for 256 bits.

A similar arguments holds for linear attacks. As for the differential uniformity, the correlation increases slowly with q according to Conjecture 1.

Conjecture 1. *If $q = p$ is a prime number, then the maximum module of the Walsh transform of $\mathcal{H}$ satisfies*

$$\max_{a \in \mathbb{F}_p^m, b \in \left(\mathbb{F}_p^m\right)^*} |\mathcal{W}_{\langle b, \mathcal{H} \rangle}(a)| \ \leq \ p \log p \ .$$

While the most general case remains a conjecture at the time of writing, this results holds for small values of p ($p \leq 71$), as can be seen in Figure 8.

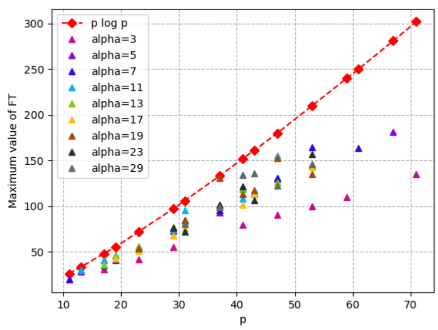

Figure 8: *The maximum value of the module of the Walsh transform of $\mathcal{H}$.*

As a consequence, it is again sufficient to activate a few S-boxes to prevent the existence of high correlation linear trails. Indeed, as established in [BSV07], a linear attack against F becomes possible when the squared modulus of $\mathcal{W}_{\langle b,F \rangle}(a)$ for some $a, b \in \mathbb{F}_q^m$ is high enough. Roughly speaking, the data complexity of a linear attack is around $1/|\mathcal{W}_{\langle b,F \rangle}(a)|^2$, so activating a few S-boxes will be sufficient for this quantity to drop below 2^{-s}, where s is the intended security level.

For both attacks, the activation of many S-boxes is further helped by our use of MDS diffusion matrices. The structure $\mathcal{M}$, based on two parallel MDS matrices $\mathcal{M}_x$ and $\mathcal{M}_y$, ensures that at least $\ell+1$ S-boxes are active in every pair of rounds.

A.2 Integral Attacks

A classical integral attack tracks the evolution of simple patterns through the rounds. Consider a function of $\mathbb{F}_q^\ell$. As explained in [BS01, BS10], a multiset of elements of $\mathbb{F}_q^\ell$ can have a word be saturated (i.e. this word takes all possible values exactly once), be constant, have a sum equal to zero, or not yield any specific pattern. These patterns are denoted "$*$", "C", "0", and "?" respectively. For example, through an S-box layer, $(*, C, ..., C)$ is mapped to $(*, C..., C)$, while the application of an MDS matrix maps $(*, C, ..., C)$ to $(*, *, ..., *)$.

In our case, such attacks do not pose a significant threat. First, the open Flystel is a 3-round Feistel network where the center round function is a permutation, so that the only integral pattern is of the form $(*, C) \rightsquigarrow (?, *)$. As a consequence, patterns at the word level cannot be propagated over two full rounds since we would need to consider open Flystel instances where one of the inputs has the ? pattern. Patterns at the open Flystel level are a bit more promising, i.e. saturating a full column using q^2 queries would lead to having fully saturated columns after one round, a patterned destroyed by the following linear layer (see [BS01, BS10] for a more thorough treatment of such generic integral attacks against SPNs).

As shown in [BCD+20], a new direction can be used in $\mathbb{F}_p$: instead of saturating a word of $\mathbb{F}_q$, it is possible instead to saturate a multiplicative subgroup. Against some algorithms like gMiMC-Hash, this approach is promising as the diffusion is slow and the only non-linear operations are monomials—under which subgroups are stable. In our case, subgroups will not be stable through an open $\texttt{Flystel}_\texttt{p}$ call because of its three internal addition/subtractions and constant additions.

In binary fields, primitives with low algebraic degree are potentially vulnerable to higher order differential cryptanalysis [Knu95], which are themselves closely related to integral attacks. The open $\texttt{Flystel}_\texttt{2}$ is an efficient counter-measure against such attacks since open butterflies operating on $(\mathbb{F}_{2^n})^2$ are known to have an algebraic degree equal to n (see Proposition 2). As shown in [BCD+20], a low degree can also be leveraged in the case where q is prime. Still, a similar argument will hold: the degree of $x \mapsto x^{1/\alpha}$ is too high to allow any meaningfull pattern to emerge.

A.3 Invariant Subspaces

Remember that, regardless of the characteristic, it always holds that $\mathcal{H}(Q_i(y), y) = (Q_f(y), y)$. For each Flystel instance in the round function (i.e., for each column in the state), the probability that an input is in this set is equal to $1/q$. As this pattern is non-linear, we deem it unlikely that it is preserved by the combination of the constant addition and the linear layer with a probability higher than chance, meaning that this pattern will be activated in inner rounds with a negligible probability.

That being said, it is a pattern that can be used to simplify the equations modeling a call to Anemoi during an algebraic attack: if an attacker has some degrees of freedom, then forcing the emergence of such a pattern within some Flystel instances is the best strategy to simplify these equations.

A.4 Number of Rounds

Based on our security analysis, we derived what we deem to be a suitable number of rounds for a given set of parameters. We plugged in the numbers and computed the numbers of rounds needed both for a security level of 128 bits (Table 5a), and of 256 bits (Table 5b). Note that the values of the digest size h and of the state size $2\ell n = 2\ell \log_2(q)$ must be coherent with the desired security level.

Table 5: *Number of Rounds of* `Anemoi`.

α	3	5	7	11	13	17
$\ell = 1$	19	19	18	18	17	16
$\ell = 2$	12	12	11	11	11	10
$\ell = 3$	10	10	10	10	10	10
$\ell = 4$	10	10	10	10	10	10

(a) *When* $s = 128$.

α	3	5	7	11	13	17
$\ell = 1$	35	35	34	34	33	32
$\ell = 2$	20	20	19	19	19	18
$\ell = 3$	15	15	15	15	15	14
$\ell = 4$	14	14	13	13	13	13

(b) *When* $s = 256$.

B Details on Algebraic Attacks

In Sections B.1 and B.2, we focus on the computation of the first Gröbner basis $\mathcal{G}_{\text{drl}}$ (Step 1) in both even and odd characteristics. Regardless of the value of q we have

$$(x_{j+1}, y_{j+1}) := \mathcal{H}(\mathcal{M}_x(x_j, y_j)[0] + c_j, \mathcal{M}_x(x_j, y_j)[1] + d_j),$$

where $\mathcal{M}_x$ is the linear layer and where $(c_j, d_j) \in \mathbb{F}_q^2$ are round constants. In Section B.3, we give details on the change of order step using FGLM (Step 2) to explain why it has been neglected in the main text.

B.1 Gröbner Basis in Characteristic 2

For even characteristic we chose $Q_i(x) = \beta x^3 + \gamma$ and $Q_f(x) = \beta x^3 + \delta$ for $\gamma \neq \delta$, so that

$$(u, v) = \mathcal{H}(x, y) \Leftrightarrow \begin{cases} (v-y)^3 + \beta y^3 + \gamma - x &= 0 \\ (v-y)^3 + \beta v^3 + \delta - u &= 0. \end{cases}$$

Assuming a linear layer of the form $\mathcal{M}_x : (x, y) \mapsto (x + gy, gx + (g^2 + 1)y)$ where g is a primitive element of $\mathbb{F}_q = \mathbb{F}_{2^n}$, the cubic equations at hand are

$$\begin{cases} f_j &:= (y_{j+1} - gx_j - (g^2+1)y_j - d_j)^3 + \beta(\alpha x_j + (g^2+1)y_j + d_j)^3 - gy_j - x_j - c_j \\ g_j &:= (y_{j+1} - gx_j - (g^2+1)y_j - d_j)^3 + \beta y_{j+1}^3 - x_{j+1}. \end{cases}$$

Experiments for Conjecture 1.

We compared the behaviour of Magma's F4 algorithm on the $\mathcal{F}_{\mathsf{CICO}}$ system for various values of n_r. In Table 6, "$d_{\text{solv}}(\mathcal{F}_{\mathsf{CICO}})$" stands for the maximal degree which occurs while computing the Gröbner basis and "Macaulay bound" is equal to $4n_r + 1$. The F4 algorithm consists in a sequence of steps, each of these steps considering all pairs of polynomials having minimal degree and treating them at the same time. Column "Step degrees" lists the degree of these steps and may provide more information than just the solving degree alone. More precisely, the "$x \to y$" indication means that the working degree of F4 increases by 1 at each step from degree x to degree y and that no *degree fall polynomials* occur, which can be considered as the expected pattern in this case. On the one hand, we see that the $\mathcal{F}_{\mathsf{CICO}}$ system seems to behave as such by looking at the sequence of step degrees. On the other hand, the solving degree grows more slowly than the Macaulay bound which is the expected bound for a random cubic system in $2n_r$ equations and more than $2n_r$ variables. Finally, the lower bound of $3n_r$ that we give in Conjecture 1 seems quite conservative regarding our results.

B.2 Gröbner Basis in Odd Characteristic

In this section, we explain why the analysis may be more complicated for odd q and we give the results of our Magma experiments to support Conjecture 2. This part is a bit

Table 6: *Gröbner basis computation on the $\mathcal{F}_{\mathsf{CICO}}$ system with $\ell = 1$ over $\mathbb{F}_{2^{15}}$.*

n_r	$d_{\text{solv}}(\mathcal{F}_{\mathsf{CICO}})$	Macaulay bound	Step degrees	Total F4 time (s)
2	8	9	$3 \to 8$	0.009
3	12	13	$3 \to 12$	0.510
4	15	17	$3 \to 15$	11.580
5	18	21	$3 \to 18$	344.050
6	21	25	$3 \to 21$	14807.639

more involved and we refer the reader to [CLO07, Bar04] for some details on Gröbner basis computation. We may consider a DRL ordering such that the largest variables are the y_i's and for which $y_{n_r} > \cdots > y_0 > x_{n_r-1} > \cdots > x_1 > x_{n_r} > x_0$. This choice is quite natural since x_0 and x_{n_r} are the fixed variables in CICO. Similarly to Appendix B.1, the expressions for f_j and g_j can be obtained from the verification equations

$$(v - y)^\alpha + \beta y^2 + \gamma - x = 0$$
$$(v - y)^\alpha + \beta v^2 + \delta - u = 0.$$

These are polynomials of degree α with leading monomial y_{j+1}^α, and their difference $h_j := g_j - f_j$ is quadratic with leading monomial y_{j+1}^2. By Buchberger's First Criterion, this implies that polynomial pairs involving equations from different rounds $i \neq j$ do not need to be treated in the first step of F4 since the leading terms are coprime. In particular, this first step only selects the pairs $\{h_j, f_j\}$ and therefore it may be relevant to analyze what happens for only one round:

Lemma 1. *A Gröbner basis for $\{h_j, f_j\}$ can be found in degree $\alpha+1$ and the set of leading terms in the reduced Gröbner basis is*

$$\zeta_j := \{y_{j+1}^2, y_j^\alpha\} \cup \{y_{j+1} x_{j+1}^u y_j^{\alpha-1-u},\ 0 \le u \le \alpha - 3\}.$$

In particular, there is one quadratic leading term and $\alpha - 1$ leading terms of degree α. The latter come from degree falls from degree $\alpha + 1$ to degree α.

Experiments for Conjecture 2.

We proceed in the same way as in Appendix B.1 to derive the following Table 7 but we do not include the Macaulay bound. Instead, we compare the behaviour of Magma's F4 on $\mathcal{F}$ and $\mathcal{F}_{\mathsf{CICO}}$ for various values of α and n_r to grasp the effect of the fixed variables. Compared to Table 6, we may also bracket the maximal degree of a polynomial in the reduced Gröbner basis in columns "$d_{\text{solv}}(\mathcal{F})$" and "$d_{\text{solv}}(\mathcal{F}_{\mathsf{CICO}})$".

A first observation is that the results for $\mathcal{F}$ and $\mathcal{F}_{\mathsf{CICO}}$ are the same when $\alpha = 3$. This might be a consequence of Lemma 1. Indeed, the leading terms in the system do not depend on the x_j variables in this case, and therefore fixing $x_0 = 0$ and $x_{n_r} = 0$ does not seem to affect the analysis. Moreover, the behaviour of the Gröbner basis algorithm seems quite close to the one on a regular system: the sequence of step degrees increases steadily until we reach the maximal degree. Also, there are no degree falls apart from the ones associated to the *plateau* at $\alpha + 1 = 4$ which are once again a consequence of Lemma 1. All seems to happen as if there were no x_j variables, so among $\{h_j, f_j\}$ one would only keep f_j since h_j expresses x_{j+1} in terms of larger variables. Also, note that the observed value $2n_r + 1$ for the maximal degree indeed corresponds to the Macaulay bound $n_r(3-1)+1$ for $\{f_0, \ldots, f_{n_r-1}\}$ assuming that it is regular.

When α grows, the behaviour of $\mathcal{F}_{\mathsf{CICO}}$ starts to deviate from the one of $\mathcal{F}$. The unusual behaviour of the computation may also be seen by looking at the sequence of step degrees

Table 7: *Gröbner basis computation on $\mathcal{F}$ and $\mathcal{F}_{\mathsf{CICO}}$ for $3 \leq \alpha \leq 11$ and for various number of rounds (odd characteristic).*

α	n_r	$d_{\text{solv}}(\mathcal{F})$	$d_{\text{solv}}(\mathcal{F}_{\mathsf{CICO}})$	Step degrees $\mathcal{F}_{\mathsf{CICO}}$
3	2	5	5(5)	3,4,4,5
	3	7	7(7)	3,4,4,5,6,7
	4	9	9(9)	3,4,4,5,6,7,8,9
	5	11	11(11)	3,4,4,5,6,7,8,9,10,11
	6	13	13(13)	3,4,4,5,6,7,8,9,10,11,12,13
5	2	10(10)	7(6)	5,6,6,6,6,7,6,6
	3	15(15)	8(8)	5,6,6,6,6,7,8,8,8,8,8,8
	4	18(18)	10(10)	5,6,6,6,6,7,8,8,8,9,9,9,9,10,10,10,10
	5		12(12)	5,6,6,6,6,7,8,8,8,9,9,9,9,10,9,10,9,10,10,11,11,11,11,12,12,12
7	2	14(14)	8(7)	7,8,8,8,8,8,8,8,8,7,7
	3		10(9)	7,8,8,8,8,8,8,9,10,10,10,10,10,10,10,10
	4		12(12)	7,8,8,8,8,8,8,9,10,10,10,10,11,11,11,12,11,12,12,12,12,12,12,12
9	2	18(18)	10(9)	
	3		13(11)	
	4		15(?)	
11	2		12(10)	
	3		15(13)	
	4		18(?)	

which is quite erratic. In particular, many degree fall polynomials at degree larger than $\alpha + 1$ occur and they imply why the solving degree remains quite low. We have not been able to analyze these degree falls at high degree. Overall, an explanation only based on simple algebraic considerations seems out of reach since it would probably be valid for any value of α while the observed results depend a lot on α. Still, it is reasonable to believe that the increased sparsity of the system for large α comes into play.

Regarding the experimental lower bound of Conjecture 2, it would be tempting to suggest an increase of d_{solv} larger than 2 at each round when α is higher, for instance 3 for $\alpha = 11$ and more generally λ_α for α where $\alpha \mapsto \lambda_\alpha$ slowly increases. However, looking at the case $\alpha = 9$ between rounds 2 and 3 and rounds 3 and 4 should not give us confidence regarding a constant increase, and also there are no theoretical arguments (for instance Hilbert series based ones) to support such a claim.

B.3 Details on the FGLM step

Regarding Step 2, the complexity of FGLM is in $\mathcal{O}\left(n_r \cdot \deg\left(I_{\mathsf{CICO}}\right)^{\omega}\right)$, where $I_{\mathsf{CICO}} := \langle \mathcal{F}_{\mathsf{CICO}} \rangle$ is the ideal generated by the system and where $\deg\left(I_{\mathsf{CICO}}\right)$ is the *degree* of this ideal.

Definition 4. Let $I \subset \mathbb{F}_q[x_0, \ldots, x_{n_r}, y_0, \ldots, y_{n_r}]$ be a zero-dimensional ideal. The degree $\deg(I)$ is defined as the dimension of $\mathbb{F}_q[x_0, \ldots, x_{n_r}, y_0, \ldots, y_{n_r}]/I$.

Note that there exists a sparse variant of FGLM [FM11] but the key quantity to grasp its complexity is still $\deg\left(I_{\mathsf{CICO}}\right)$. Also, for some arithmetization-oriented primitives, the cost of this step was even estimated by $\mathcal{O}\left(n_r \cdot \deg\left(I_{\mathsf{CICO}}\right)\right)$, see for instance [BSGL20, Appendix, p.12]. We are not aware of the techniques employed to derive this result; in particular, this bound might underestimate the real cost in the case of Anemoi.

Characteristic 2.

Using the generic Bezout bound for a system of $2n_r$ cubic equations, we obtain

$$\deg\left(I_{\mathsf{CICO}}\right) \leq 3^{2n_r} \ .$$

Also, from experiments it seems that this bound is tight as we always have $\deg\left(I_{\mathsf{CICO}}\right) = 3^{2n_r}$. Therefore, we estimate the complexity of Step 2 to be $\mathcal{O}(n_r \cdot 3^{2n_r})$ with $\omega = 1$, and this is much smaller than the one obtained for Step 1.

Odd characteristic.

For Step 2 as well, the situation is slightly more complicated in odd characteristic. Indeed, the Bezout bound yields $\deg\left(I_{\mathsf{CICO}}\right) \leq 2^{n_r}\alpha^{n_r}$ while the observed degree is much smaller:

Conjecture 3 (Degree, odd characteristic)**.** *We have* $deg\left(I_{\mathsf{CICO}}\right) \leq (\alpha+2)^{n_r}$.

We are able to prove Conjecture 3 “by hands" for $n_r = 1$ and an investigation of the general case is left for future work. Actually, even by adopting the Bezout bound instead of Conjecture 3 as well as $\omega = 2$, a very rough upper-bound for Step 2 is $\mathcal{O}(n_r^2 \cdot 2^{2n_r} \cdot \alpha^{2n_r})$, and similarly this is already quite below the cost of Step 1.

C Reference Implementation

A full reference implementation of `Anemoi`, including `AnemoiJive` and `AnemoiSponge`, is provided in our GitHub[9] repository. It contains various routines to evaluate these functions and to generate the corresponding systems of equations as well. Nevertheless, we include some snippets from this implementation below. First, we provide the linear layers.

```
def M_2(x_input, b):
    """Adapted from a pseudo-Hadamard transform"""
    x = x_input[:]
    x[0] += b*x[1]
    x[1] += b*x[0]
    return x

def M_3(x_input, b):
    """Adapted from figure 6 of [DL18]."""
    x = x_input[:]
    t = x[0] + b*x[2]
    x[2] += x[1]
    x[2] += b*x[0]
    x[0] = t + x[2]
    x[1] += t
    return x


def M_4(x_input, b):
    """Adapted from figure 8 of [DL18]."""
    x = x_input[:]
    x[0] += x[1]
    x[2] += x[3]
    x[3] += b*x[0]
    x[1]  = b*(x[1] + x[2])
    x[0] += x[1]
    x[2] += b*x[3]
    x[1] += x[2]
    x[3] += x[0]
    return x

def circulant(field, l):
    for row in itertools.combinations_with_replacement(range(0,l+1), l):
        mat = matrix.circulant(list(row)).change_ring(field)
        if is_mds(mat):
            return mat
```

The, the following function computes the number of rounds.

```
def get_n_rounds(s, l, alpha):
    """Returns the number of rounds needed in Anemoi (based on the
    complexity of algebraic attacks).

    """
    r = 0
    complexity = 0
    while complexity < 2**s:
        r += 1
        complexity = binomial(
            2*l*r + alpha + 1 + 2*(l*r-2),
            2*l*r
        )**2
    r += l+1 # security margin
    if r > 10:
        return r
    else:
        return 10
```

[9] https://github.com/vesselinux/anemoi-hash

Finally, the two modes in which `Anemoi` can be plugged are implemented by the following function. They both take an input `P` which must implement a permutation. Concretely, it must be such that calling `P(x)` on a list `x` of elements of the relevant field returns a list of elements of the same field of the same size.

```
def jive(P, b, _x):
    """Returns an output b times smaller than _x using the Jive mode of
    operation and the permutation P.

    """
    if b < 2:
        raise Exception("b must be at least equal to 2")
    if P.input_size() % b != 0:
        raise Exception("b must divide the input size!")
    x = _x[:]
    u = P(x)
    compressed = []
    c = P.input_size()/b # length of the compressed output
    for i in range(0, c):
        compressed.append(sum(x[i+c*j] + u[i+c*j]
                              for j in range(0, b)))
    return compressed

def sponge_hash(P, r, h, _x):
    """Uses Hirose's variant of the sponge construction to hash the
    message x using the permutation P with rate r, outputting a digest
    of size h.

    """
    x = _x[:]
    if P.input_size() <= r:
        raise Exception("rate must be strictly smaller than state size!")
    # message padding (and domain separator computation)
    if len(x) % r == 0 and len(x) != 0:
        sigma = 1
    else:
        sigma = 0
        x += [1]
        x += (len(x) % r)*[0]
    padded_x = [[x[pos+i] for i in range(0, r)]
                for pos in range(0, len(x), r)]
    # absorption phase
    internal_state = [0] * P.input_size()
    for pos in range(0, len(padded_x)):
        for i in range(0, r):
            internal_state[i] += padded_x[pos][i]
        internal_state = P(internal_state)
        if pos == len(padded_x)-1:
            # adding sigma if it is the last block
            internal_state[-1] += sigma
    # squeezing
    digest = []
    pos = 0
    while len(digest) < h:
        digest.append(internal_state[pos])
        pos += 1
        if pos == r:
            pos = 0
            internal_state = P(internal_state)
    return digest
```